27
6/16/77 & NTIS
25 cop

UCID- 17486

Lawrence Livermore Laboratory

Alfvén-Ion-Cyclotron Instability in Mirror Machines

D. C. Watson, L. D. Pearlstein, L. L. Lodestro

May 24, 1977

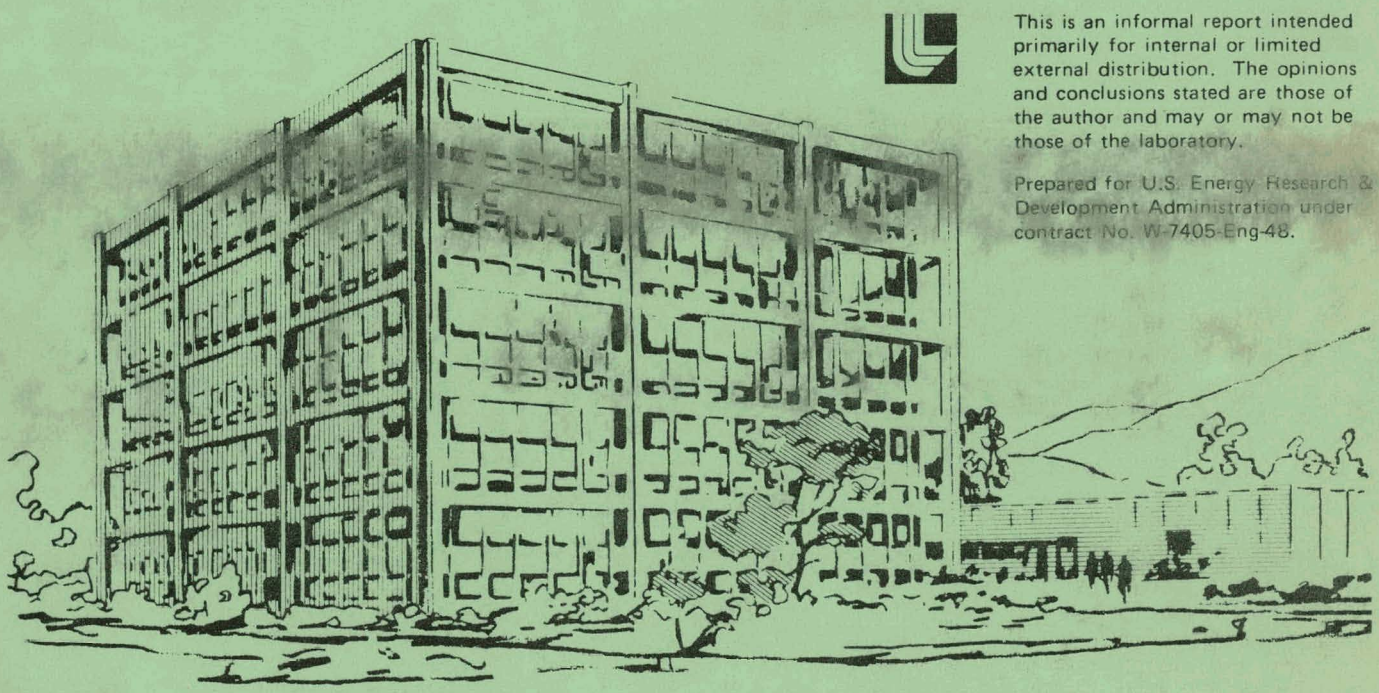

This is an informal report intended primarily for internal or limited external distribution. The opinions and conclusions stated are those of the author and may or may not be those of the laboratory.

Prepared for U.S. Energy Research & Development Administration under contract No. W-7405-Eng-48.

MASTER

DISTRIBUTION OF THIS DOCUMENT IS UNLIMITED

DISCLAIMER

This report was prepared as an account of work sponsored by an agency of the United States Government. Neither the United States Government nor any agency Thereof, nor any of their employees, makes any warranty, express or implied, or assumes any legal liability or responsibility for the accuracy, completeness, or usefulness of any information, apparatus, product, or process disclosed, or represents that its use would not infringe privately owned rights. Reference herein to any specific commercial product, process, or service by trade name, trademark, manufacturer, or otherwise does not necessarily constitute or imply its endorsement, recommendation, or favoring by the United States Government or any agency thereof. The views and opinions of authors expressed herein do not necessarily state or reflect those of the United States Government or any agency thereof.

DISCLAIMER

Portions of this document may be illegible in electronic image products. Images are produced from the best available original document.

Alfvén-Ion-Cyclotron Instability in Mirror Machines*

D. C. Watson, L. D. Pearlstein, L. L. Lodestro

Abstract

Electrostatic instabilities occurring in mirror-confined ion velocity-distributions have been thoroughly investigated. The electromagnetic instability of greatest concern is the Alfvén-ion-cyclotron (AIC) mode. In this work we investigate both convective and absolute growth, both in homogeneous plasma and in finite machines, for a variety of ion velocity-distributions. Good agreement is found with the results from the particle simulation code "Superlayer". Quasilinear effects are outlined and a rough criterion found for the importance of Dupree-type broadening.

NOTICE

This report was prepared as an account of work sponsored by the United States Government. Neither the United States nor the United States Energy Research and Development Administration, nor any of their employees, nor any of their contractors, subcontractors, or their employees, makes any warranty, express or implied, or assumes any legal liability or responsibility for the accuracy, completeness or usefulness of any information, apparatus, product or process disclosed, or represents that its use would not infringe privately owned rights.

*Work performed under the auspices of the U.S. Energy Research and Development Administration under contract No. W-7405-Eng-48.

DISTRIBUTION OF THIS DOCUMENT IS UNLIMITED

MASTER

ALFVÉN-ION-CYCLOTRON INSTABILITY IN MIRROR MACHINES

D. C. Watson, L. D. Pearlstein, L. L. Lodestro

I. Influence of Mode on Machine Design

II. Approximations Used in Study of Mode

III. AIC Stability Boundaries for Tractable Ion Distributions

IV. Relation to the Superlayer Code

V. Distributions of the Holdren Type

VI. Distributions Whose Angular Spread is a Function of Velocity

VII. Numerically Specified Distributions

VIII. Diffusion and Stabilization

I. Influence of Mode on Mirror Machine Design

Electrostatic instabilities occurring in mirror-confined ion velocity-distributions[1,2] have been thoroughly investigated. The high-frequency convective mode places an upper limit on machine length.[3] The drift-cyclotron-loss-cone mode places a large lower limit on machine radius, so that in 2X this mode requires a plasma stream for additional stabilization.[4] Both of these modes are driven by population inversion in perpendicular velocity.

The study of electromagnetic instabilities occurring in mirror-confined ion distributions is still in progress. Of greatest concern is the Alfvén-ion-cyclotron (AIC) mode.[5,6] This instability, unlike the HF convective instability, can become absolute; further, the shift from convective to absolute[7] occurs at modest β-values and anisotropy-values (e.g. $\beta \sim 0.5$ for $T_\perp : T_\parallel \sim 2:1$).[8] Stabilization via finite machine-length thus is achieved not by limiting the convective amplification but rather by spatially confining the mode sufficiently[9] to depress its absolute growth rate. This is a more severe restriction, in general. The AIC instability, unlike the drift-cyclotron-loss-cone instability, does not require a hole in the perpendicular velocity distribution. Thus addition of a cool-plasma stream is not effective in stabilizing it. Finite machine-width introduces an effective perpendicular wavevector and a radial gradient in field and density. We can explain the absence of violent AIC instability in the 2X machine by invoking the short scale-length of the plasma in terms of ion Larmor radii, which leads to a discrete set of allowable modes with reduced growth rate, together with the short scale-radius which introduces a non-zero $k_\perp$ into the AIC dispersion relation. The effect of radial gradients has not yet been examined.

II. Approximations Used in Study of Mode

The approximations that are made in the study of AIC instability fall into three main groups: approximations to the macroscopic form of the plasma, approximations to the microscopic form of the ion velocity distribution, and approximations to the kinematics of the mode itself. The first and second groups are of course related via the equilibrium ion dynamics; the first and third groups are of course related via restrictions on the possible wavevectors and polarizations.

The actual plasma has variation along and across the magnetic field lines. The longitudinal variation is treated in the WKB approximation. We ignore the detailed perpendicular variation from one field line to the next; instead we study AIC propagation on a single "representative" field line. The perpendicular variation in plasma properties we plan to include in future to lowest order by locating the single "representative" field line in a linear transverse gradient. The finite perpendicular extent we approximate by requiring a non-zero $k_\perp$.

Recent work on the perpendicular differential equation satisfied by the field amplitude[10] suggests that the value of $k_\perp$ in question is around $k_\perp^2 a_i R_p = 1$.

We adopt the more conservative assumption that a transverse mode pattern exists which roughly accommodates a half-wavelength within the diameter of the plasma, so that

$$x \equiv \frac{k_\perp^2 a_{i\perp}^2}{2} = \frac{\pi^2}{8} \frac{a_{i\perp}^2}{R_p^2} \tag{1}$$

There remains the choice of a characteristic Larmor radius and characteristic plasma radius. The MX plasma is expected to have a relatively uniform central region surrounded by a relatively narrow sheath or edge region which is 1 or 2 Larmor radii wide. For MX, therefore, it makes sense to take R_p to be the distance from the axis out to this sheath and to take for $a_{i\perp}$ its central axis value. The 2X plasma, on the other hand, is all sheath; the falloff in density from the axis can be modeled as a Gaussian and the characteristic length taken to be the scale length of this Gaussian; the Larmor radius should be taken intermediate between axis and edge values and for lack of any stricter guide we take the geometric mean for convenience. The axis and edge values of the ion Larmor radius are taken from the long thin approximation.

Before describing the longitudinal variation problem in detail, we recall that the AIC mode in homogeneous plasma can be either convective or absolute. As an example, for a bimaxwellian ion distribution with a temperature anisotropy of 2:1 the transition from convective to absolute behavior occurs at a β-value of 0.6. At a β-value infinitesimally less than this, the convective growth length for 7 exponentiations is about 30 ion Larmor radii. For less severe anisotropy the transition occurs at higher β and vice versa, but the length of homogeneous plasma required for substantial convective growth is always a few tens of Larmor radii and this remains true for other types of ion distribution. Thus 2X and the end plugs of TMX are too short for convective AIC instability to be a separate issue. Only absolute AIC instability need be considered. In MX and the central tank of TMX, on the other hand, the convective AIC growth may constitute a problem at β values too low for absolute instability.

What corresponds to absolute instability when the plasma has longitudinal variation? The answer is a discrete series of spatially-confined temporally-

growing mode-patterns. Each is characterized by a frequency ω and by spatial turning points $s = \pm s_T$ measured from the symmetry plane of the machine such that[9]

$$\int_{-s_T}^{s_T} ds \left[\frac{k_{\parallel}^{+}(s) - k_{\parallel}^{-}(s)}{2} \right] = (2n + 1)\pi \qquad n = 0,1,2 \ldots \tag{2}$$

and such that the roots $k_{\parallel}^{+}(s)$, $k_{\parallel}^{-}(s)$ of the AIC dispersion relation coincide at $s = \pm s_T$, which requires

$$\left. \frac{d\omega}{dk_{\parallel}} \right|_{s = \pm s_T} = 0 \tag{3}$$

The WKB approximation is based on $\frac{dk}{dx} << k^2$, which implies that the value of the integer n in (2) should be large. However the growth rates furnished by (2) increase with decreasing n, so that the most important mode from the viewpoint of stable machine operation is also the one for which the growth rate estimate is the least reliable, namely $n = 0$.

The dependence of the wave numbers $k_{\parallel}^{\pm}$ on position is further approximated by

$$k_{\parallel}^{\pm}(s) = k_o \pm \delta k \tag{4}$$

$$\delta k^2 = \frac{\partial\left(k-k_o\right)^2}{\partial\omega} \left(\omega-\omega_o\right) + \frac{\partial\left(k-k_o\right)^2}{\partial B} \left(B(s) - B(0)\right) \tag{5}$$

where $\left(\omega_o, k_o\right)$ satisfy the criteria for absolute instability in a homogeneous plasma with the properties of the plasma at $s = 0$. Finally we make the approximation

$$B(s) = B(0)\left(1 + \frac{s^2}{L^2}\right) \tag{6}$$

The validity of the approximations (5) and (6) can only be checked a posteriori, since they must hold all the way to the turning points $\pm s_T$ whose positions are not known at first. Indeed, the value of L in (6) may be chosen to vary with s_T in a (not strictly correct) attempt to deal with the following forms of B(s) dependence:[11]

(A) Ion injection localized near midplane, moderate to high β:

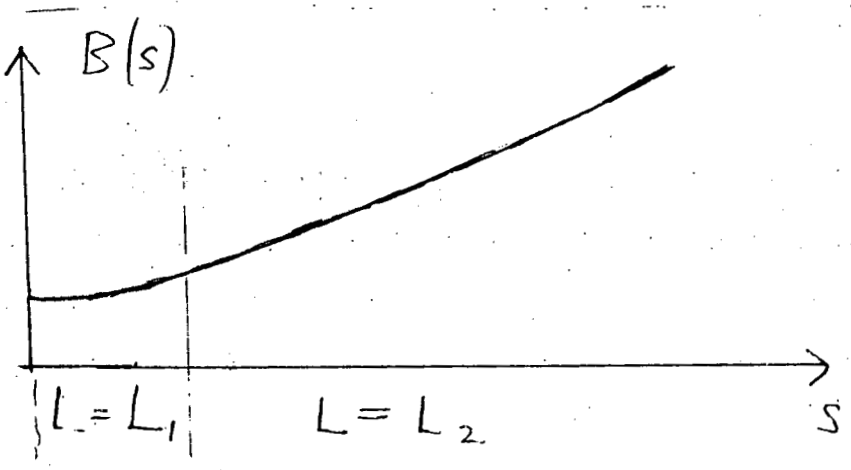

$L_1 < L_2$

Fig. (1)

(B) Ion injection uniform over broader region, moderate to high β:

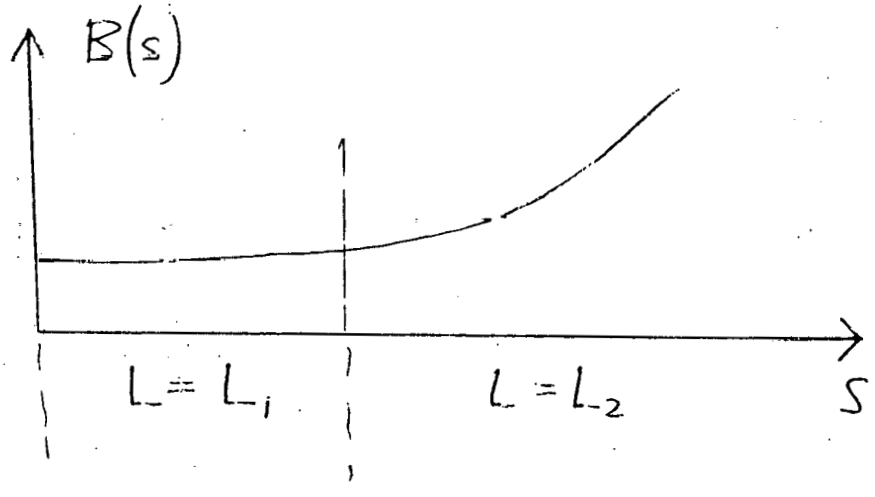

$L_1 > L_2$

Fig. (2)

The long thin approximation is used to relate internal and external mirror-ratios. The ambipolar potential is approximated by a linear B-dependence:

$$\Phi(B) = \frac{B_{throat} - B}{B_{throat} - B_{center}} \Phi\left(B_{center}\right) \tag{7}$$

We plan to estimate convective growth in a plasma with spatial variation along a field line by calculating the quantity

$$A\left(\omega_{re}\right) = \exp\left\{\int ds\ k_{\parallel im}\left(\omega_{re}, s\right)\right\} \tag{8}$$

where the integral is carried out along that field line. The real frequencies ω_{re} will be scanned to find the worst-case spatial amplification. This calculation is important for the central tank of TMX and may be important for MX.

Now let us consider the approximations made in the ion velocity distribution. The dependence on B is that required by the adiabatic constant of motion $v_\perp^2/B$. Non-adiabaticity[12] is ignored. In cases where the ambipolar potential is negative, such as the central cell of a triple-mirror,[13] the ambipolar hole joining the loss cones is replaced by an ambipolar plug separating the loss-cones. This makes the dispersion function harder to evaluate, and so we neglect the potential for a quick conservative estimate of the β-limit in the central tank. In general, wherever possible, we work with analytically tractable distributions having at worst the form

$$f_o(v_\perp, v_\parallel) = \frac{1}{n!}\frac{\alpha_{o\perp}}{\pi}\sqrt{\frac{\alpha_{o\parallel}}{\pi} + \frac{\alpha_{o\perp}}{\pi\left(R_{oc}-1\right)}}\, e^{-\alpha_{o\perp}v_\perp^2 - \alpha_{o\parallel}v_\parallel^2 + \alpha_{o\perp}v_{oh}^2}$$

$$\cdot\ \alpha_{o\perp}^n\left[v_\perp^2 - \frac{v_\parallel^2}{R_{oc}-1} - v_{oh}^2\right]^n \equiv F\left(v_\perp, v_\parallel, \alpha_{o\perp}, \alpha_{o\parallel}, v_{oh}, R_{oc}\right) \tag{9}$$

at the center plane and the form

$$f(v_\perp, v_\parallel) = F\left(v_\perp, v_\parallel, \alpha_\perp, \alpha_\parallel, v_h, R_c\right)\left(\frac{\alpha_{o\perp}}{\alpha_\perp}\right)^{n+1} \sqrt{\frac{B}{B_o}} \left(\frac{R_c - 1}{R_{oc} - 1}\right)^{n + \frac{1}{2}}$$

$$\cdot \exp\left\{\left(2\left(\Phi_o - \Phi\right) - \left(\frac{B}{B_o} - 1\right)v_{oh}^2\right)\left(\alpha_{o\perp} + \left(R_{oc} - 1\right)\alpha_{o\parallel}\right)/\left(R_{oc} - \frac{B}{B_o}\right)\right\} \tag{10}$$

at other points along the "representative" field-line. In (10)

$$\alpha_\perp = \left(\alpha_{o\perp} + \left(\frac{B}{B_o} - 1\right)\alpha_{o\parallel}\right) \cdot \frac{B_o}{B} \qquad R_c = R_{oc}\, B_o/B$$

$$\alpha_\parallel = \alpha_{o\parallel} \qquad v_h^2 = \frac{\left(R_{oc} - 1\right)v_{oh}^2 - 2\left(\Phi_o - \Phi\right)}{R_c - 1} \tag{11}$$

The distribution in (9) is normalized to unity. The equation (9) is the simplest way to combine a loss-cone, an ambipolar hole, and a marked pressure anisotropy over and above that introduced by the previous two features. We neglect the detailed behavior of the electrons and take the ambipolar potential as given by (7). To prevent the loss-hyperboloid of one sheet in (9) from becoming a loss-hyperboloid of two sheets in (10), which would greatly complicate the AIC dispersion function, we require

$$v_h^2 \geq 0 \qquad v_{oh}^2 \geq \frac{2\left(\Phi_o - \Phi_{throat}\right)}{R_{oc} - 1} \tag{12}$$

Then the coefficient of F in (10) is just the density normalized to the density at the midplane.

The "tractable distributions" of type (9) are capable of reproducing closely the numerical output of Fokker-Planck codes, with and without DCLC turbulence.[4] Without turbulence[14] the appearance of the Fokker-Planck output

is that of a bimaxwellian, cut by a ramp which slopes down to zero at the loss-hyperboloid:

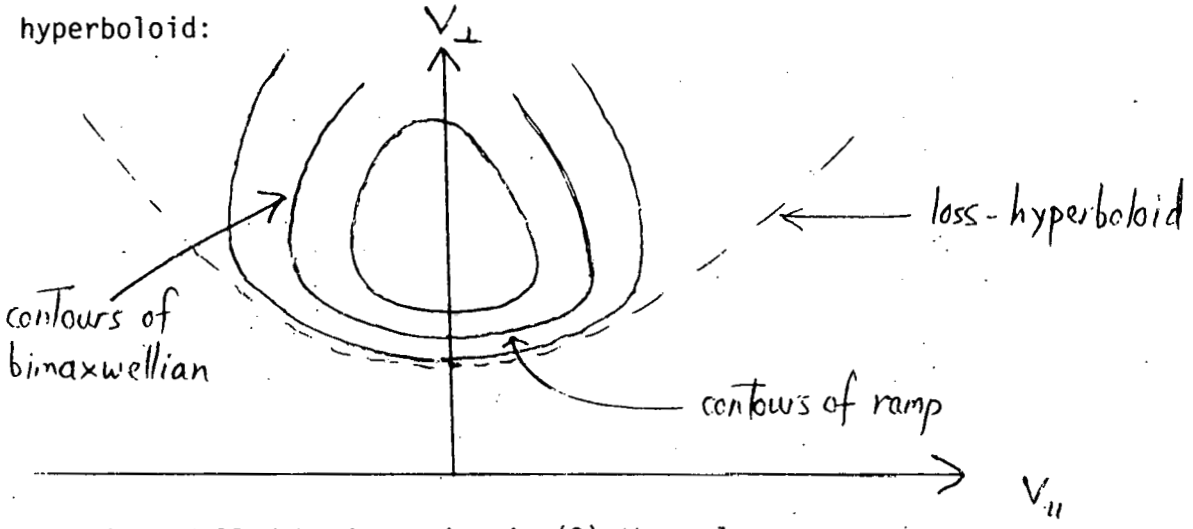

Fig. (3)

This is modelled by inserting in (8) the values

$$\alpha_{o\perp} < \alpha_{o\parallel} \qquad v_{oh} \neq 0 \qquad n = 1 \qquad R_{oc} = B_{throat}/B_o \tag{13}$$

With turbulence and narrow-angle injection[15] the appearance of the Fokker-Planck output is that of a high aspect-ratio bimaxwellian, somewhat distorted and attenuated within the loss-hyperboloid:

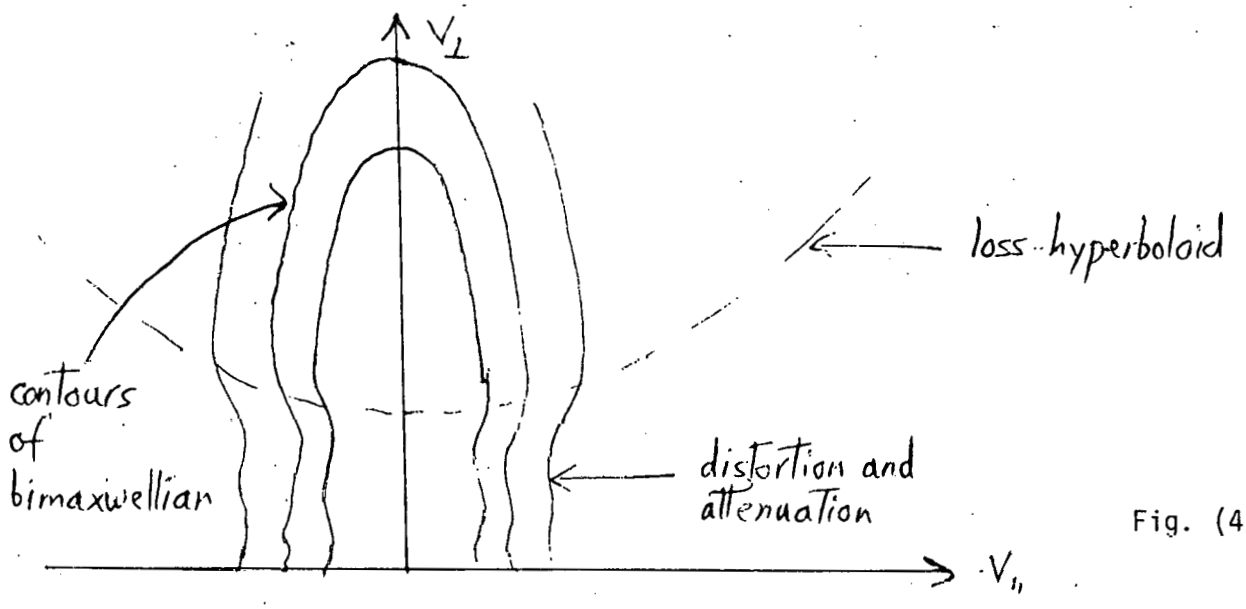

Fig. (4)

This is modelled by inserting in (9) the values

$$\alpha_{o\perp} < \alpha_{o\parallel} \qquad v_{oh} = 0 \qquad n = 0 \qquad R_{oc} = \infty \tag{14}$$

With turbulence and wide-angle injection, the appearance of the Fokker-Planck output is approximated by a linear combination of the distributions appearing in Figs. (3) and (4). The effect of the turbulence is merely to fill in the ambipolar hole, not to broaden the ion distribution in $v_{\parallel}$. This is because the Fokker-Planck code models turbulence due to DCLC. Since the DCLC mode is perpendicularly polarized and is electrostatic, it has a diffusion tensor

$$\vec{\vec{D}} \sim \langle \vec{E}_{\perp} \vec{E}_{\perp} \rangle \tag{15a}$$

which is incapable of diffusing particles in $v_{\parallel}$. The effect of turbulence due to the AIC mode itself is discussed in Section VIII. The AIC mode is perpendicularly polarized and electromagnetic. Thus its diffusion tensor has a component

$$D_{\parallel\parallel} \sim v_{\perp} \times B_{\perp} \cdot v_{\perp} \times B_{\perp} \tag{15b}$$

which can diffuse ions in the $v_{\parallel}$-direction.

These tractable distributions are the natural candidates for work on exact phase-integrals and work on gradient effects. The bimaxwellian has already been used to estimate the effect of finite transverse extent on the AIC mode.

Considerable time has been spent on other, more complicated distribution functions. For these, the AIC dispersion function requires numerical integration, and correspondingly its repeated evaluation requires large amounts of computer time. These distributions fall into three main classes: the Holdren-type distributions,[16] dominated by ion-ion collisions; distributions whose angular extent is a function of velocity,[8] chosen to model the combined effect of electron drag and ion-ion collisions on an injected beam; and numerically specified distributions furnished directly by Fokker-Planck codes.[14,15] These distributions will be described in more detail in those sections devoted to them.

Finally let us consider the approximations made in the kinematics of the mode itself. The mode in its simplest description[5,6] propagates in the direction of the magnetic field in a homogeneous plasma, and is a purely left-hand circularly-polarized wave. It has the dispersion relation

$$0 = \underbrace{\frac{k_\parallel^2 c^2}{\omega_{pi}^2}}_{\text{free-space contribution}} + \underbrace{\frac{\omega}{\omega_{ci}}}_{\text{electron contribution approximated by EXB drift}} + \underbrace{\frac{\omega}{\omega - \omega_{ci}}}_{\text{ion cold-fluid contribution}} + \underbrace{\int d^3v \, \frac{k_\parallel v_\parallel \frac{\omega}{\omega - \omega_{ci}} f_o}{\omega - k_\parallel v_\parallel - \omega_{ci}}}_{\text{ion isotropic non-fluid contribution}}$$

$$- \underbrace{\int d^3v \, k_\parallel v_\parallel \frac{f_o + v_\perp^2 \frac{\partial f_o}{\partial v_\parallel^2}}{\omega - k_\parallel v_\parallel - \omega_{ci}}}_{\text{ion anisotropy contribution}} \qquad (16)$$

The ω^2 term in the free-space contribution is due to displacement current and has been neglected. The form of the electron contribution is justified because the frequency is much lower than the electron cyclotron frequency and the wave length is much longer than the electron Larmor radius.

Introducing a non-zero $k_\perp$ means that one has to equate the determinant of the dispersion tensor to zero. With cool electrons and low frequencies the parallel electric field is almost shorted out, which motivates the following treatment of the dispersion tensor. Starting from

$$\begin{pmatrix} D_{LL} & D_{LR} & D_{LZ} \\ D_{RL} & D_{RR} & D_{RZ} \\ D_{ZL} & D_{ZR} & D_{ZZ} \end{pmatrix} \cdot \begin{pmatrix} E_L \\ E_R \\ E_Z \end{pmatrix} = \begin{pmatrix} 0 \\ 0 \\ 0 \end{pmatrix} \qquad (17)$$

substitute for E_Z and obtain

$$\begin{pmatrix} D_{LL} - D_{LZ}\, D_{ZL}/D_{ZZ} & D_{LR} - D_{LZ}\, D_{ZR}/D_{ZZ} \\ D_{RL} - D_{RZ}\, D_{ZL}/D_{ZZ} & D_{RR} - D_{RZ}\, D_{ZR}/D_{ZZ} \end{pmatrix} \bullet \begin{pmatrix} E_L \\ E_R \end{pmatrix} = \begin{pmatrix} 0 \\ 0 \end{pmatrix} \tag{18}$$

Neglecting the second term in each element of the matrix (17) is equivalent to neglecting the parallel electric field E_Z. On computing those terms one finds that they may be neglected provided that

$$\frac{T_e}{T_i} \ll \beta \quad \text{and} \quad \frac{T_e}{T_i} \ll 1 \tag{19}$$

Here β is the local β which is of order unity or greater for most cases of interest. The ratio T_e/T_i is around 10^{-2} for 2X, MX and the end-plugs of TMX, thus for these machines one may approximate the oblique dispersion relation for the AIC mode by coupling to the right-hand (whistler) mode only:

$$D_{LL}\, D_{RR} - D_{LR}\, D_{RL} = 0 \tag{20}$$

For the central tank of TMX, on the other hand, parallel-propagating ion-sound waves can also couple to the AIC mode, so that one must use for the oblique AIC dispersion relation the full determinantal equation

$$\left(D_{LL} - D_{LZ}\, D_{ZL}/D_{ZZ}\right)\left(D_{RR} - D_{RZ}\, D_{ZR}/D_{ZZ}\right) - \left(D_{LR} - D_{LZ}\, D_{ZR}/D_{ZZ}\right)\left(D_{RL} - D_{RZ}\, D_{ZL}/D_{ZZ}\right) = 0 \tag{21}$$

One more complication occurs in the kinematics. When modeling the perpendicular structure of an AIC disturbance by a non-zero $k_\perp$, one must examine how the Bessel-function argument (1) varies along a field-line. If one neglects fanning due to quadrupole fields, and assumes that the transverse mode structure remains tied to field-lines, one can see that to lowest order the argument

(1) is independent of B for a delta-function velocity-distribution and varies like B for an isotropic Maxwellian (unconfined) distribution. For continuous distributions which are partly or wholly confined, the variation of (1) with B is slower than linear and has been neglected.

III. AIC Stability Boundaries for Tractable Ion Distributions

In equation (9) we set out a class of center-plane ion distributions which allowed for a loss-cone, an ambipolar hole and a pressure anisotropy over and above that introduced by the previous two features. These features are quantitatively related for this class of distributions as follows

$$\underbrace{\frac{P_{o\perp}}{P_{o\parallel}} - 1}_{\text{total pressure anisotropy}} = \underbrace{\frac{1}{R_{oc} - 1}\left(\frac{3}{2} + n + \alpha_{o\perp} v_{oh}^2\right)}_{\text{loss-cone-angle contribution}} + \underbrace{\alpha_{o\perp} v_{oh}^2}_{\text{ambipolar hole contribution}}$$

$$+ \underbrace{\left(\frac{\alpha_{o\parallel}}{\alpha_{o\perp}} - 1\right)\left(1 + n + \alpha_{o\perp} v_{oh}^2\right)}_{\text{two-temperature contribution}} + \underbrace{n}_{\text{contribution of slope down to loss-hyperboloid}} \tag{22}$$

This class of distributions is convenient for analytic work.

It is useful to first review some infinite plasma results. On substituting (9) in (16), the AIC parallel-propagation dispersion-relation assumes the form, convenient for computation,

$$0 = D(K_\parallel, W) \equiv \frac{K_\parallel^2}{\tilde{\beta}_o} + \frac{W^2}{W-1} + \frac{1}{2}\,\frac{1}{R_{oc} - 1}\left(\xi_o^2 Z'(\xi_o) - 1\right)$$

$$+ \frac{1}{2}\left[\frac{1}{W-1} + \frac{\alpha_{o\parallel}}{\alpha_{o\perp}}\left(1 + n + H_o^2\right) + \frac{1}{R_{oc} - 1}\left(n + H_o^2\right)\right] Z'(\xi_o) \tag{23}$$

The quantities appearing in this dispersion function are normalized to the magnetic field, plasma density, and total plasma pressure at the center-plane of the machine, as follows

$$\left.\begin{aligned}
&K_{\parallel} = k_{\parallel}/\omega_{cio}\sqrt{\alpha_o^{phys}} \qquad < \alpha_o^{phys}\, v_i^2 > \;\equiv\; \frac{3}{2} \qquad \omega_{cio} = \frac{Z_i e\, B_o}{m_i} \\
&W = \omega/\omega_{cio} \qquad H_o^2 = \alpha_{o\perp} v_{oh}^2 \\
&\tilde{\beta}_o = \frac{2n_i m_i \mu_o <v_i^2>}{3B_o^2} \qquad \xi_o = \frac{W-1}{K_{\parallel}}\sqrt{\frac{\tilde{\beta}_o}{\tilde{\beta}_{\parallel o}}} \\
&\tilde{\beta}_{\parallel o} = \frac{2n_i m_i \mu_o <v_{\parallel i}^2>}{B_o^2} = \frac{\beta_{\parallel o}}{1 - \beta_{\perp o}}
\end{aligned}\right\} \qquad (24)$$

The condition for absolute instability is[7] that there exist $(K_{\parallel o}, W_o)$ such that

$$\left.\begin{aligned}
&\mathrm{Im}(W_o) > 0 \\
&D(K_{\parallel o}, W_o) = 0 \\
&\frac{\partial D(K_{\parallel o}, W_o)}{\partial K} = 0
\end{aligned}\right\} \qquad (25)$$

and such that the coincident roots in K migrate to infinity on opposite sides of the real K-axis as W goes to infinity in the positive imaginary direction. The derivative of D in (25), as well as additional derivatives required by the Newton-Raphson routine which finds the solution of (25), are taken numerically so that the analytic expression (23) suffices.

Given as input $\beta_{\parallel o}$, $\beta_{\perp o}$, and n, one may use (22) to find any one of R_{oc}, $\alpha_{o\parallel}/\alpha_{o\perp}$, and $\alpha_{o\perp} v_{oh}^2$ in terms of the other two. This allows one to explore

the two-dimensional space of macroscopic plasma parameters $\beta_\perp$ and $\beta_\parallel$ (or alternatively average β and anisotropy-ratio) while holding to some hypothesis regarding the microscopic structure of the ion velocity distribution. For instance, one may set $R_{oc} = \infty$, $n = 0$, $\overline{v^2_{oh}} = 0$, and explore the stability of the AIC mode as a function of β and pressure anisotropy for the case of a bimaxwellian ion distribution. One may set $v^2_{oh} = 0$, $\alpha_{o\perp}/\alpha_{o\parallel} = 1$, $n = 0$, and explore the stability of the AIC mode, again in the 2-dimensional β-anisotropy domain, for the case of a sharp-cutoff loss-cone ion distribution. In fact these two types of distribution represent some kind of extrema for the AIC mode. Barring quite pathological types of velocity distribution e.g. with particles piled up against the loss boundary, it is found that for most reasonable distributions the AIC mode is less stable than in the bimaxwellian case and more stable than in the sharp loss-cone distribution. It is unfortunate that the behavior of the mirrormode is just the opposite, at least for center-plane onset.

When exploring the $\beta_\perp$ - $\beta_\parallel$ plane in the manner described above, one must bear in mind that for $n > 0$ the relation (22) restricts the areas of the plane that can be reached.

To make the above clearer, we show graphs of the $\beta_\perp$ - $\beta_\parallel$ plane on which are marked the AIC convective-absolute transition and the onset of the mirrormode. Figure (5) is drawn for a bimaxwellian distribution, Fig. (6) for a sharp loss-cone.

The computer code that traces out the boundary incorporates two important running checks: a check that the topological criterion following (25) is satisfied and a check on the importance of convective growth.

5A

5

ALFVÈN-ION-CYCLOTRON MODE, CONVECTIVE-ABSOLUTE TRANSITION, AND MIRRORMODE CRITERION, CENTERPLANE ONSET; BIMAXWELLIAN DISTRIBUTION.

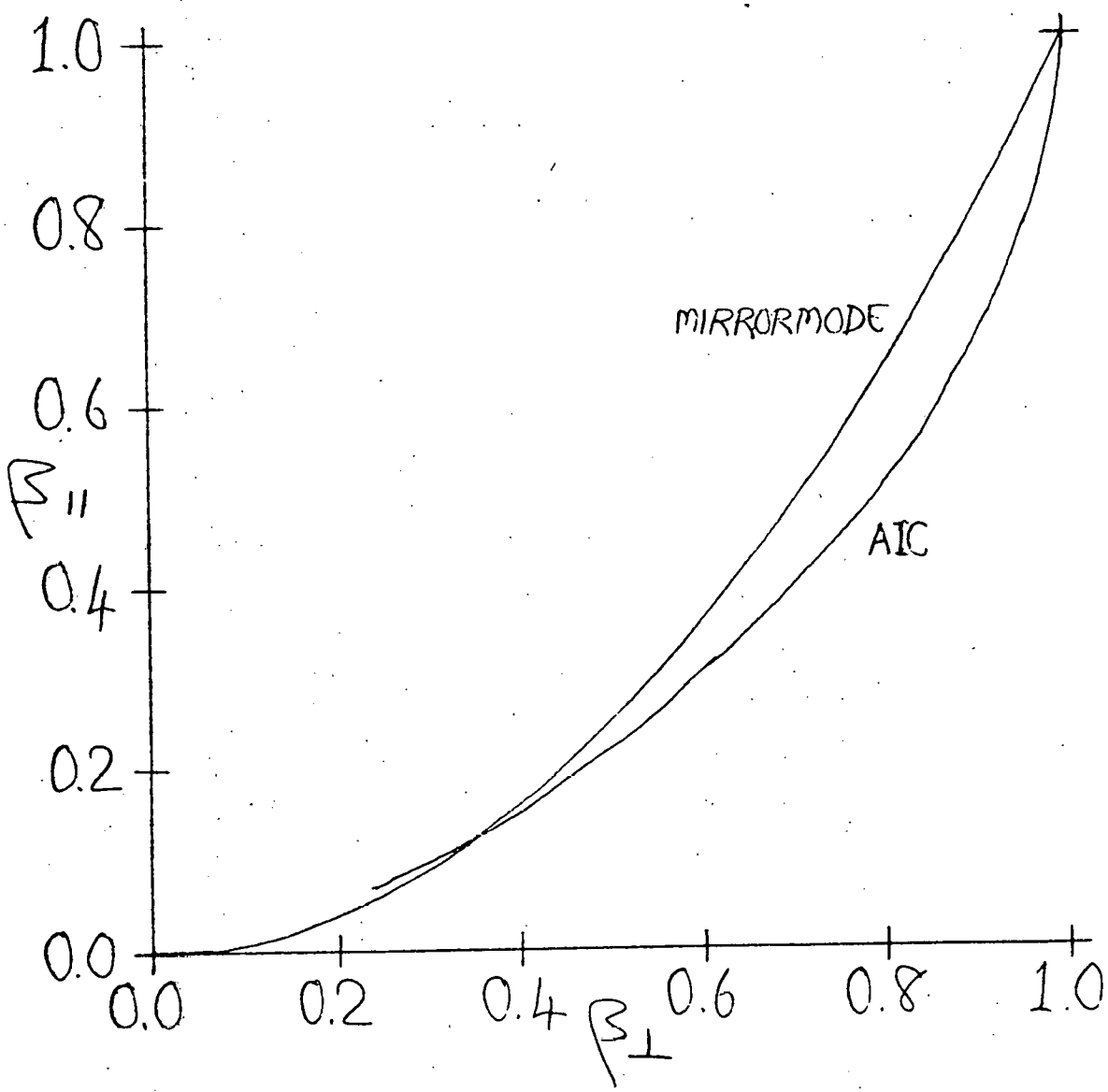

MACHINE VACUUM MIRROR RATIO IS 2:1

6. ALFVÈN-ION-CYCLOTRON MODE, CONVECTIVE-ABSOLUTE TRANSITION, AND MIRRORMODE CRITERION, CENTERPLANE ONSET, CUT-MAXWELLIAN DISTRIBUTION.

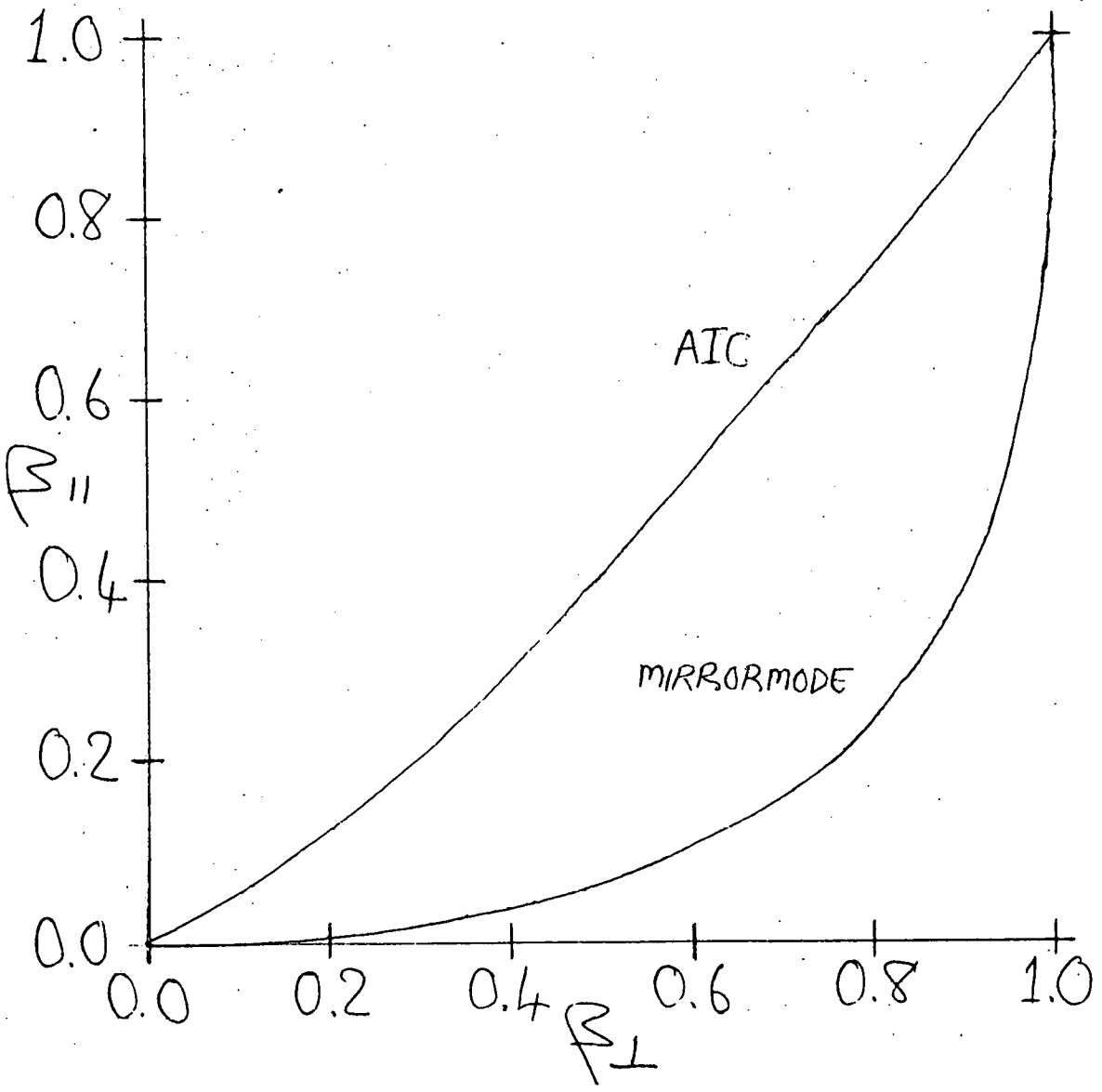

MACHINE VACUUM MIRROR RATIO IS 2 : 1

Two analytic results which are not only physically interesting but also useful for checking codes are the limits of the AIC dispersion relation for high and zero anisotropy. The high-anisotropy limit is the fluid limit, as can be seen by referring to the definition of ξ_0 in (24). Using the asymptotic expansion of the Z′-function in (23) and the relation between parameters expressed in (22), one obtains the fluid AIC dispersion relation in normalized form

$$0 = \frac{K^2}{\tilde{\beta}_0} + \frac{W^2}{W-1} + \frac{3}{4}\,\frac{K^2}{(W-1)^2} \tag{26}$$

This dispersion relation applies to any highly anisotropic ion distribution. The zero-anisotropy form of (23) is even more easily obtained

$$0 = \frac{K^2}{\tilde{\beta}_0} + \frac{W^2}{W-1} + \frac{1}{2}\,\frac{W}{W-1}\,Z'\left(\frac{W-1}{K}\right) \tag{27}$$

This dispersion relation does not apply to arbitrary isotropic distributions.

We now move on to the effects of finite plasma radius. We use Equation (20) to study 2X and MX, and invoke a non-zero perpendicular wavevector (see (1) and the accompanying discussion).

We regard the value of $k_\perp$ as a given real parameter, as if characterizing the perpendicular mode pattern in a wave guide. We proceed to look for convective or absolute growth in the parallel spatial direction. From this point on, the problem is one-dimensional. The right-hand side of (23) is replaced by a somewhat more complicated expression, namely, the result of substituting a bimaxwellian ion distribution in the left-hand side of (20) and normalizing according to (24).

This expression is treated as a dispersion function relating W and $K_\parallel$, with $K_\perp$ entering as a parameter. Explicitly (23) is replaced by

$$D(K_{\parallel}, W) = \left\{ \frac{K_{\parallel}^2}{\tilde{\beta}_0} + \frac{K_{\perp}^2}{2\tilde{\beta}_0} + W + \sum_{\ell=-1}^{1} Z_{o\ell} X_{\ell}^{LL} \right\}$$

$$\cdot \left\{ \frac{K_{\parallel}^2}{\tilde{\beta}_0} + \frac{K_{\perp}^2}{2\tilde{\beta}_0} - W + \sum_{\ell=-1}^{1} Z_{o\ell} X_{\ell}^{RR} \right\} \qquad (28)$$

$$- \left\{ \frac{K_{\perp}^2}{2\tilde{\beta}_0} + \sum_{\ell=-1}^{1} Z_{o\ell} X_{\ell}^{LR} \right\}^2$$

$$Z_{o\ell} \equiv \frac{W}{W-\ell} + \frac{1}{2} \left(\frac{W}{W-\ell} - 1 + \frac{\alpha_{o\parallel}}{\alpha_{o\perp}} \right) Z'(\xi_o^{\ell})$$

$$\xi_o^{\ell} \equiv \frac{W-\ell}{K_{\parallel}} \sqrt{\frac{\tilde{\beta}_0}{\tilde{\beta}_{\parallel o}}} \qquad (29)$$

$$X_{\ell}^{LL} = -\left(\frac{x}{2} - \ell\right) \Gamma_{\ell-1} + (x - \ell)\, \Gamma_{\ell} - \frac{x}{2} \Gamma_{\ell+1}$$

$$X_{\ell}^{RR} = -\frac{x}{2} \Gamma_{\ell-1} + (x + \ell)\, \Gamma_{\ell} - \left(\frac{x}{2} + \ell\right) \Gamma_{\ell+1}$$

$$X_\ell^{RL} = \frac{x}{2}\,\Gamma_{\ell-1} - x\,\Gamma_\ell + \frac{x}{2}\,\Gamma_{\ell+1}$$

$$\Gamma_\ell = I_\ell\,(x)\,e^{-x} \qquad x = \frac{k_\perp^{\,2}\,a_{i\perp}^{\,2}}{2} = \frac{\pi^2}{8}\,\frac{(a_{i\perp}^{vacuum})^2}{R_p^{\,2}\,(1-\beta_\perp)^\alpha} \tag{29}$$

$$K_\perp^2 = 2x\,\frac{\tilde{\beta}_o}{\tilde{\beta}_{\perp o}}$$

where we take $\alpha = \frac{1}{2}$ for 2X

and $\alpha = 1$ for MX as discussed in Section II,

and where the definitions (24) are again employed.

The results of exploring AIC stability in the $\beta_\perp$ - $\beta_\parallel$ plane then appear as in Figure (7). The convective-absolute boundary is shifted to allow higher anisotropy at a given β. The boundary curves over at high β because the ratio of machine width to Larmor radius decreases swiftly there.

We now move on to the effects of finite plasma length. We use (1) through (6) to obtain the following estimate for the growth rate depression due to finite length

$$\Delta W = \frac{-1}{D_W}\sqrt{\left[\frac{R_o^{vac}}{\sqrt{1-\beta_\perp}} - 1\right]\frac{D_{\tilde{B}}}{1-\beta_\perp}\,\frac{\beta_o}{\beta_{o\perp}}\,\frac{D_{KK}}{2\,\hat{L}_{well}^2}} \tag{30}$$

Subscripts on D indicate derivatives which are all taken at the center plane. The derivative with respect to $\tilde{B}$ includes the self-consistent density variation. This estimate is in terms of the normalized quantities (24) with the addition of

$$\tilde{B} \equiv B/B_o$$
$$\hat{L}_{well} \equiv L_{well}/a_{i\perp}^{vac} \tag{31}$$

CONVECTIVE-ABSOLUTE BOUNDARIES FOR 2X, MX, AND INFINITE PLASMA. FINITE-WIDTH EFFECT ONLY.
BI-MAXWELLIAN ION VELOCITY DISTRIBUTION

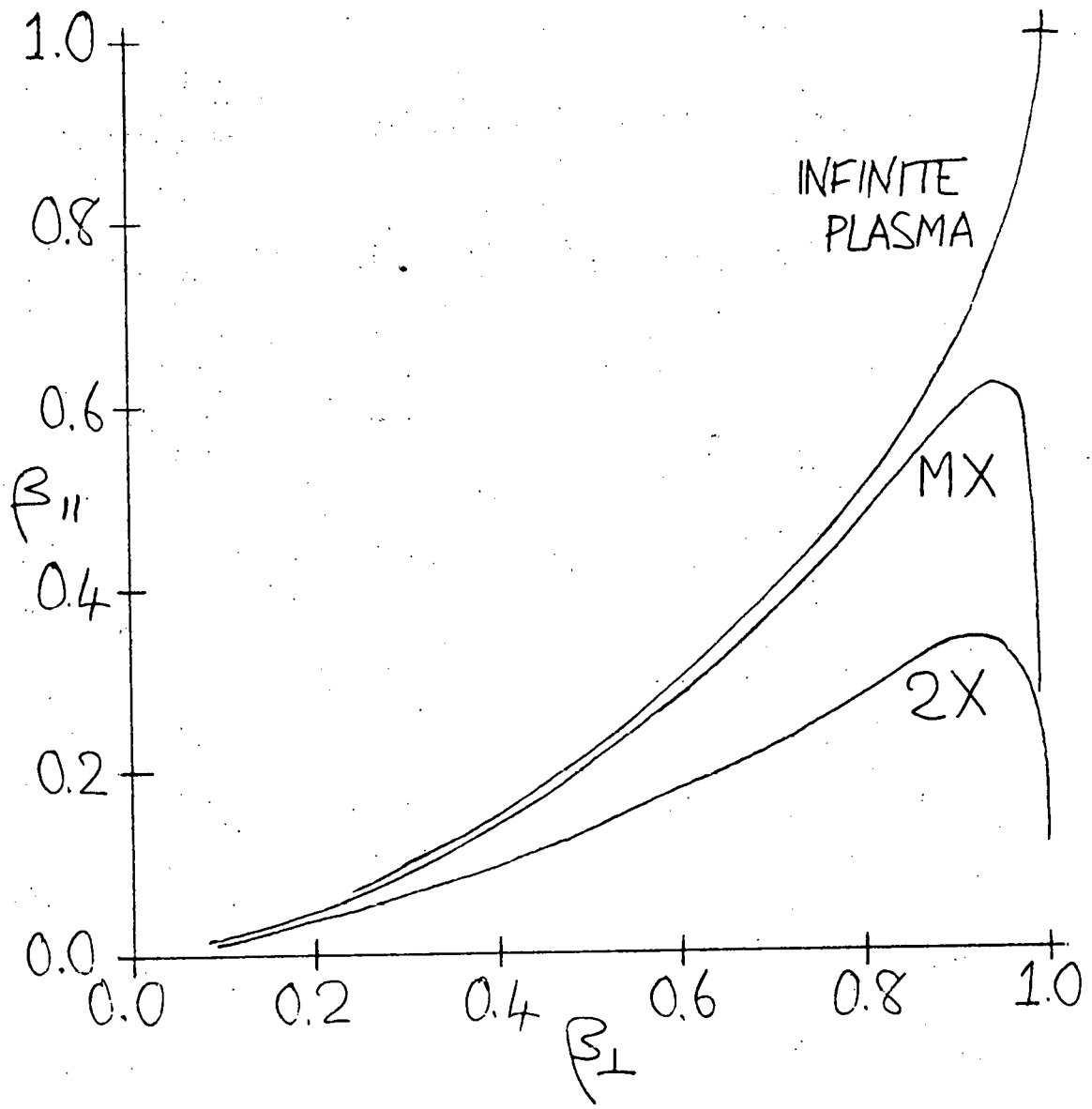

2X : $R_p = 2.7\, a_i^{vacuum}$ $L_B = \infty$

MX : $R_p = 15\, a_i^{vacuum}$ $L_B = \infty$

Again the long thin approximation has been used. (6) has been fitted to the requirement that

$$B(L_{well}) = B_{throat}$$
$$B(o) = B_{vac}\sqrt{1-\beta_\perp} \tag{32}$$

The derivative with respect to $\tilde{B}$ is taken numerically. This requires finding the AIC dispersion function for parallel propagation, away from the midplane, which is obtained by substituting (10) in (16). Denote the coefficient of F in (10), which is the density relative to the midplane density, by N. Then

$$D(K_\parallel, W) = \frac{K_\parallel^2}{\tilde{\beta}_o} + N\left\{\frac{W^2}{\tilde{B}(W-\tilde{B})} + \frac{1}{2}\frac{1}{R_c-1}(\xi^2 Z'(\xi) - 1)\right.$$
$$\left. + \frac{1}{2}\left[\frac{\tilde{B}}{W-\tilde{B}} + \frac{\alpha_\parallel}{\alpha_\perp}(1 + n + H^2) + \frac{1}{R_c-1}(n + H^2)\right] Z'(\xi)\right\} \tag{33}$$

The quantities appearing here are defined by (11) and (24) with the addition of

$$\xi = \frac{W-\tilde{B}}{K_\parallel}\sqrt{\frac{\tilde{\beta}_o}{\tilde{\beta}_{\parallel o}}}\sqrt{\frac{R_{oc}-1}{R_{oc}-\tilde{B}}} \qquad H^2 = \alpha_\perp v_h^2 \tag{34}$$

Graphs similar to Fig. (5) and Fig. (6) may now be obtained with (30) taken into account. The results are shown in Figures (8) and (9).

8

CONVECTIVE-ABSOLUTE BOUNDARIES FOR 2X, MX AND INFINITE PLASMA. FINITE-LENGTH EFFECTS ONLY. BI-MAXWELLIAN ION VELOCITY DISTRIBUTION.

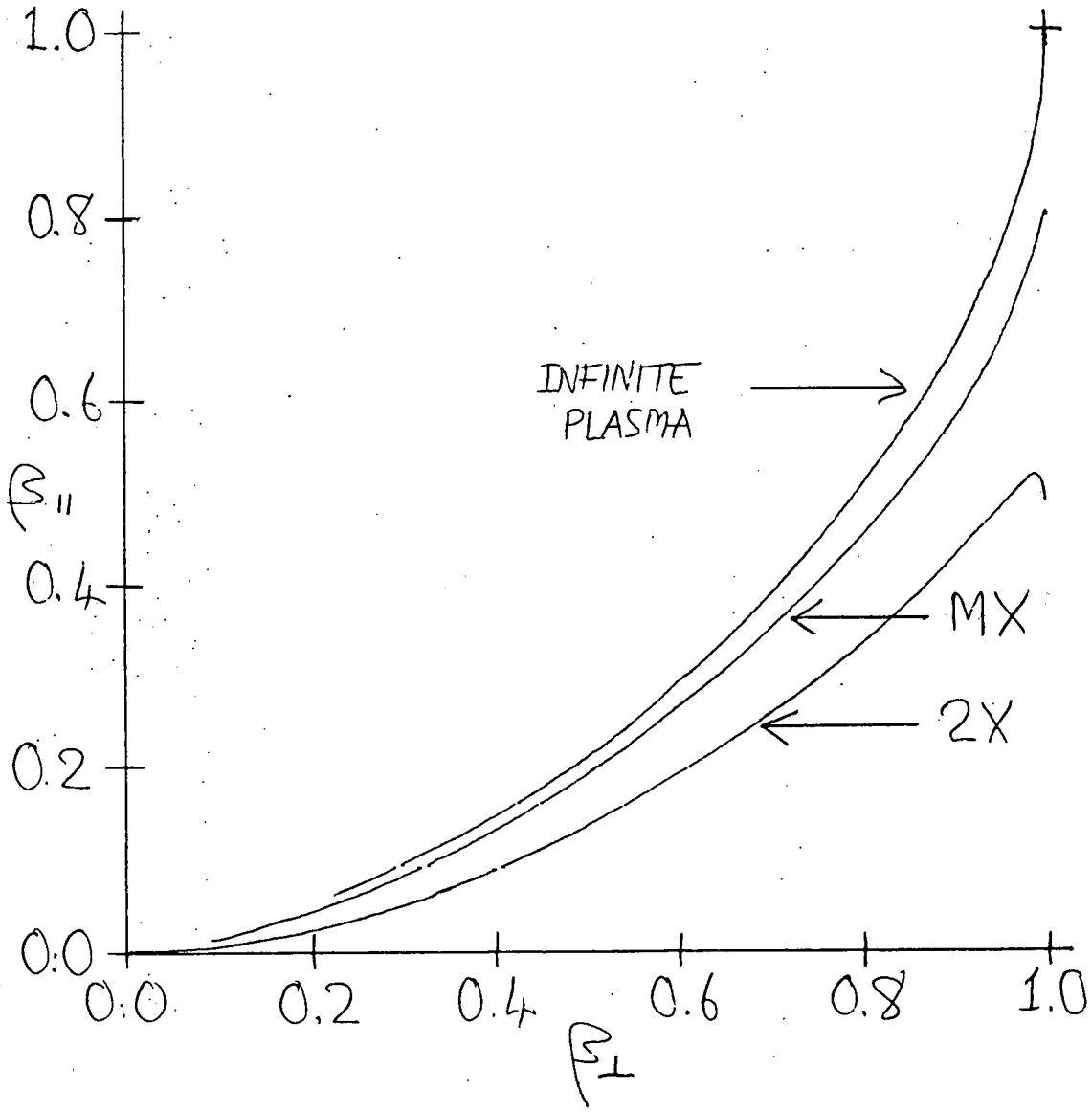

$2X: \; R_p = \infty \qquad L_B^{vacuum} = 15\, a_i^{vacuum}$

$MX: \; R_p = \infty \qquad L_B^{vacuum} = 50\, a_i^{vacuum}$

CONVECTIVE-ABSOLUTE BOUNDARIES FOR 2X, MX AND INFINITE PLASMA. FINITE-LENGTH EFFECT ONLY.

CUT-MAXWELLIAN ION VELOCITY DISTRIBUTION.

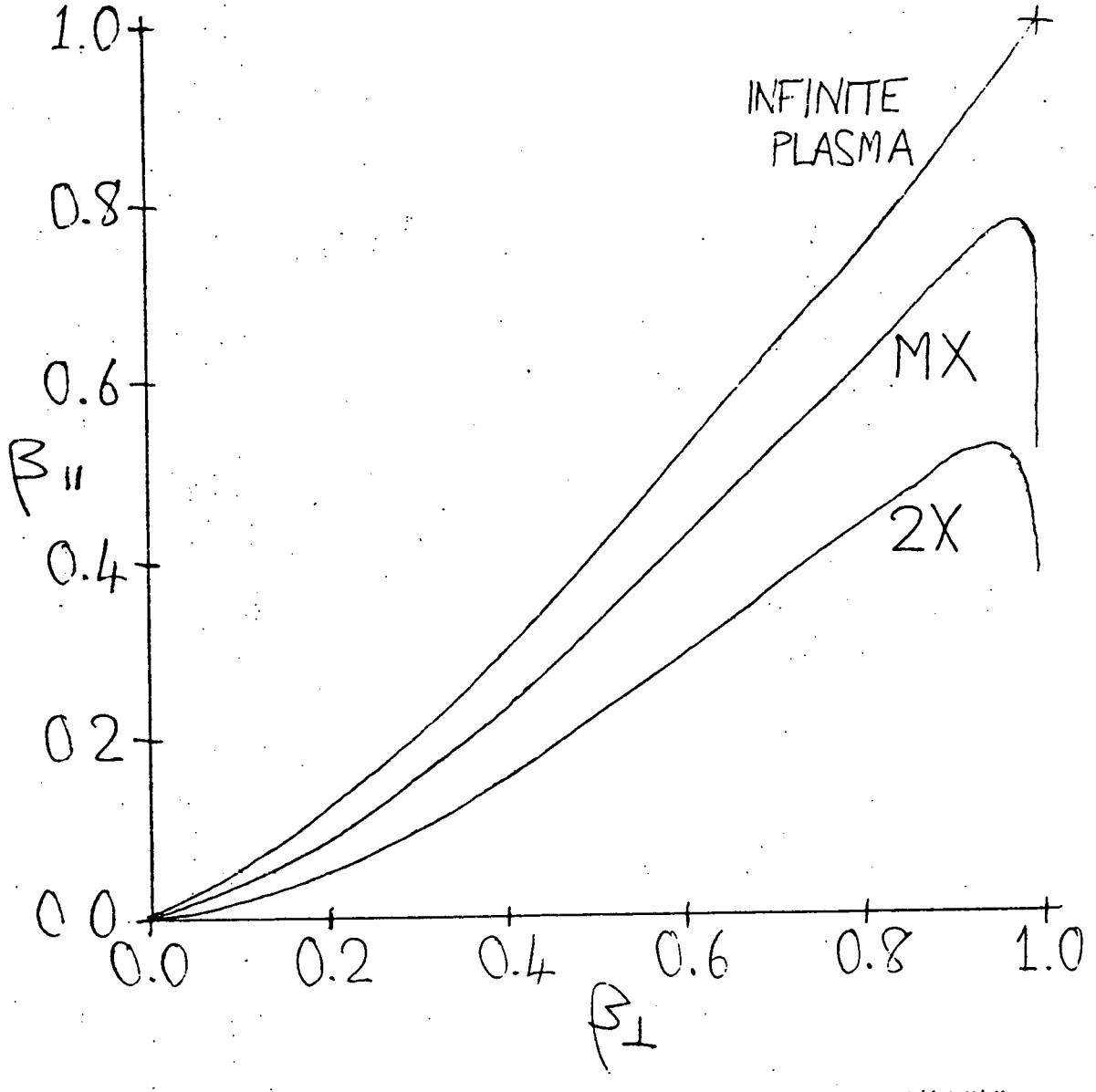

2X : $R_p = \infty$ $\quad L_B^{vacuum} = 15\, a_i^{vacuum}$

MX : $R_p = \infty$ $\quad L_B^{vacuum} = 50\, a_i^{vacuum}$

Finally, we compute the convective-absolute boundary in $\beta_\perp$ - $\beta_\parallel$ space bringing in both finite-width and finite-length stabilization. The expression (30) for the finite-length growth-rate depression is employed. The function D is that displayed in (28), except that for calculating the numerical derivative with respect to $\tilde{B}$ one requires the off-center-plane form

$$
\begin{aligned}
D(K_\parallel, W) = & \left\{ \frac{K_\parallel^2}{\tilde{\beta}_0} + \frac{K_\perp^2}{2\tilde{\beta}_0} + N \left[\frac{W}{\tilde{B}} + \sum_{\ell=-1}^{1} Z_\ell \, X_\ell^{LL} \right] \right\} \\
& \bullet \left\{ \frac{K_\parallel^2}{\tilde{\beta}_0} + \frac{K_\perp^2}{2\tilde{\beta}_0} + N \left[- \frac{W}{\tilde{B}} + \sum_{\ell=-1}^{1} Z_\ell \, X_\ell^{RR} \right] \right\} \\
& - \left\{ \frac{K_\perp^2}{2\tilde{\beta}_0} + N \left[\sum_{\ell=-1}^{1} Z_\ell \, X_\ell^{LR} \right] \right\}^2
\end{aligned}
\tag{35}
$$

$$
Z_\ell = \frac{W}{W-\ell\tilde{B}} + \frac{1}{2} \left(\frac{W}{W-\ell\tilde{B}} - 1 + \frac{\alpha_\parallel}{\alpha_\perp} \right) Z'(\xi^\ell)
$$

$$
\xi^\ell = \frac{W-\ell B}{K_\parallel} \sqrt{\frac{\tilde{\beta}_0}{\tilde{\beta}_{\parallel 0}}}
$$

The rationale for using the same values of X and x as at the mid-plane was discussed at the end of Section II. The convective-absolute boundaries obtained are displayed in Figure (10).

CONVECTIVE - ABSOLUTE BOUNDARIES FOR 2X, MX AND INFINITE PLASMA.
FINITE-WIDTH AND FINITE-LENGTH EFFECTS.
BI-MAXWELLIAN ION VELOCITY DISTRIBUTION

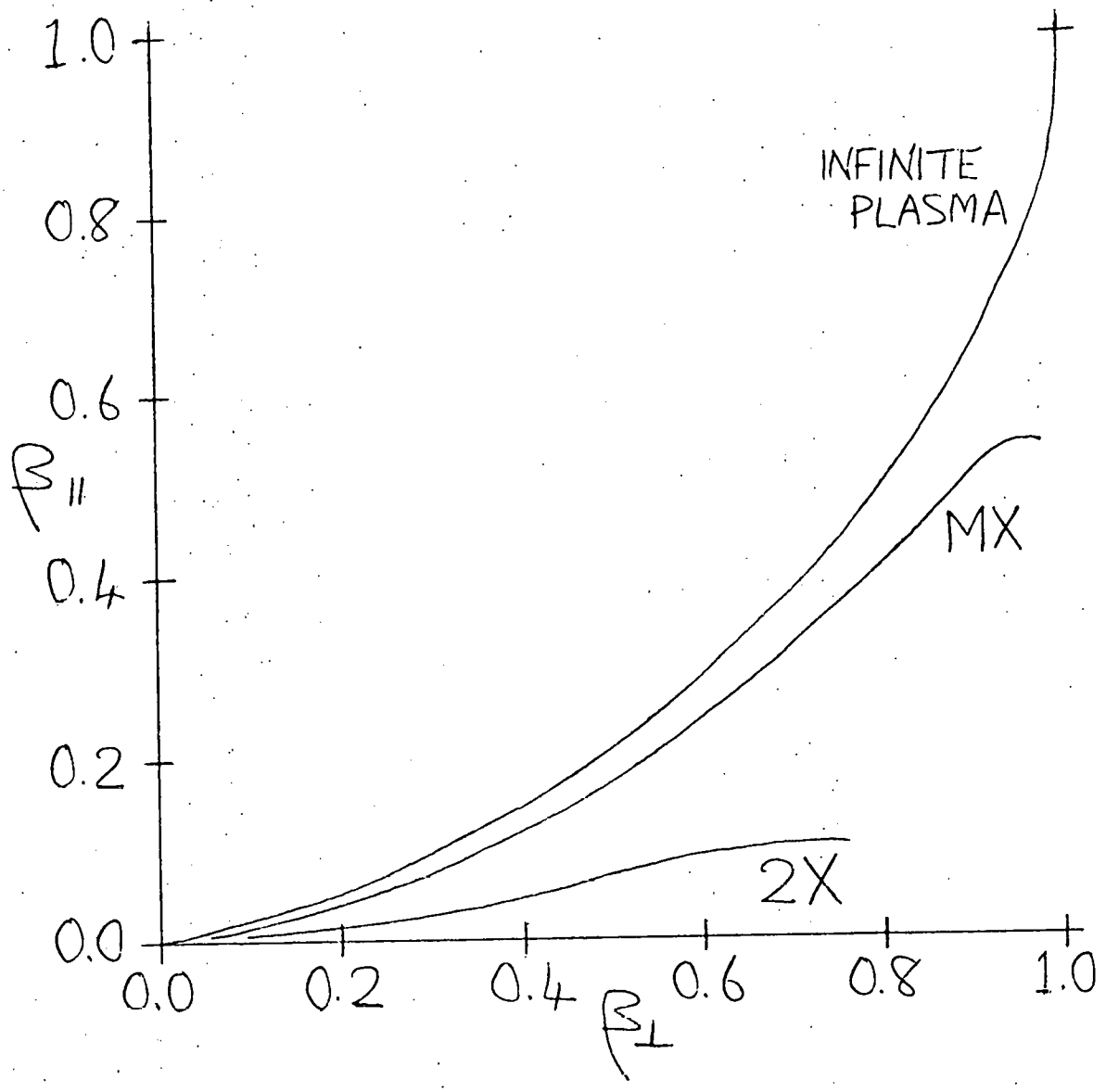

2X : $R_p = 2.7\, a_i^{vacuum}$ $\quad L_B^{vacuum} = 15\, a_i^{vacuum}$

MX : $R_p = 15\, a_i^{vacuum}$ $\quad L_B^{vacuum} = 50\, a_i^{vacuum}$

IV. Relation to the Superlayer Code

In Section III the stability of the AIC mode was examined in finite plasmas similar to those occuring in real and projected experimental devices. In this section the stability of the AIC mode will be examined in "plasmas" of the type occurring in particle simulations, in particular simulations of the "Superlayer" series.[17] We show a good agreement between the dispersion-relation-based predictions of the $\beta_\perp$ - $\beta_\parallel$ graphs and the actual stable or unstable behavior of the "Superlayer" computer runs. This agreement strengthens our confidence in the predictions of the $\beta_\perp$ - $\beta_\parallel$ graphs for stable or unstable operations in the MX device.

The main differences between the experimental plasmas and the Superlayer "plasmas" studied are four in number. Firstly, the Superlayer runs studied are 1-dimensional in the direction of the magnetic field so effectively the "plasma" has infinite width. Secondly, the "plasma" is set up to be very short - usually between 1 and 5 Larmor radii in length. Thirdly, there is no self-consistent magnetic field depression - the equilibrium magnetic field is constant and the ions are contained by an effective "potential". Fourthly, the electric field polarization is constrained to be linear. Let us see how these differences are reflected in the computation of stability boundaries in the $\beta_\perp$ - $\beta_\parallel$ plane.

Firstly, the finite-width dispersion-function (35) is ruled out, and all computations are restricted to the parallel-propagation dispersion-function (33).

Secondly, the finite-length stabilization is strong so that the stability boundaries lie in regions of high anisotropy (e.g. one may attain $\beta_\perp : \beta_\parallel = 10 : 1$ at $\beta_\perp = 0.5$ if given a plasma 1 Larmor orbit long).

Thirdly, the WKB estimate of growthrate depression (30) must be revised to

$$\Delta W = -\frac{1}{D_W}\sqrt{D_N \frac{\beta_o}{\beta_\perp} \frac{D_{KK}}{2\tilde{L}_N^2}} \tag{36}$$

Here D_N indicates a derivative with respect to density alone. The form of the bimaxwellian velocity distribution is not affected by the effective "potential"; only the density varies along the field line as exp $(-Z^2/L_N^2)$ say. The magnitude of the B-field as mentioned earlier is artifically held constant. Thus the definition $\tilde{L}_N = L_N/a_{i\perp}$ needs no reference to a vacuum field, and the stability boundary for fixed $\tilde{L}_N$ does not curve over at high $\beta_\perp$.

Fourthly, one must find the form of D in an artificial universe where current in only one perpendicular direction acts as a source of the vector potential. This form is

$$D_{artificial}(K_\parallel, W) = \frac{1}{2}\{D(K_\parallel, W) + D(-K_\parallel, -W)\} \tag{37}$$

Here the D on the right-hand-side is that of (33) with $\tilde{B} = 1$ but with N allowed to vary for purposes of taking the numerical derivative in (36).

The appearance of the resulting graphs in the $\beta_\perp$ - $\beta_\parallel$ plane is shown in Fig. (11). Points in $\beta_\perp$ - $\beta_\parallel$ space corresponding to specific Superlayer runs are marked together with the values of $\tilde{L}_N$ employed and the observation or non-observation of AIC instability. The agreement is remarkably good and strengthens our belief that diagrams like Fig. (10) are an appropriate guide to the choice of device parameters for stable operation.

Ideally one would wish to recompute the boundaries appearing in Fig. (10) using more suitable ion velocity distributions, exact parallel phase integrals,

1

CONVECTIVE-ABSOLUTE BOUNDARIES FOR DENSITY HUMP WITHOUT MAGNETIC WELL. BI-MAXWELLIAN ION VELOCITY DISTRIBUTION. CONSTRAINED LINEAR POLARIZATION.

"1-D SUPERLAYER"

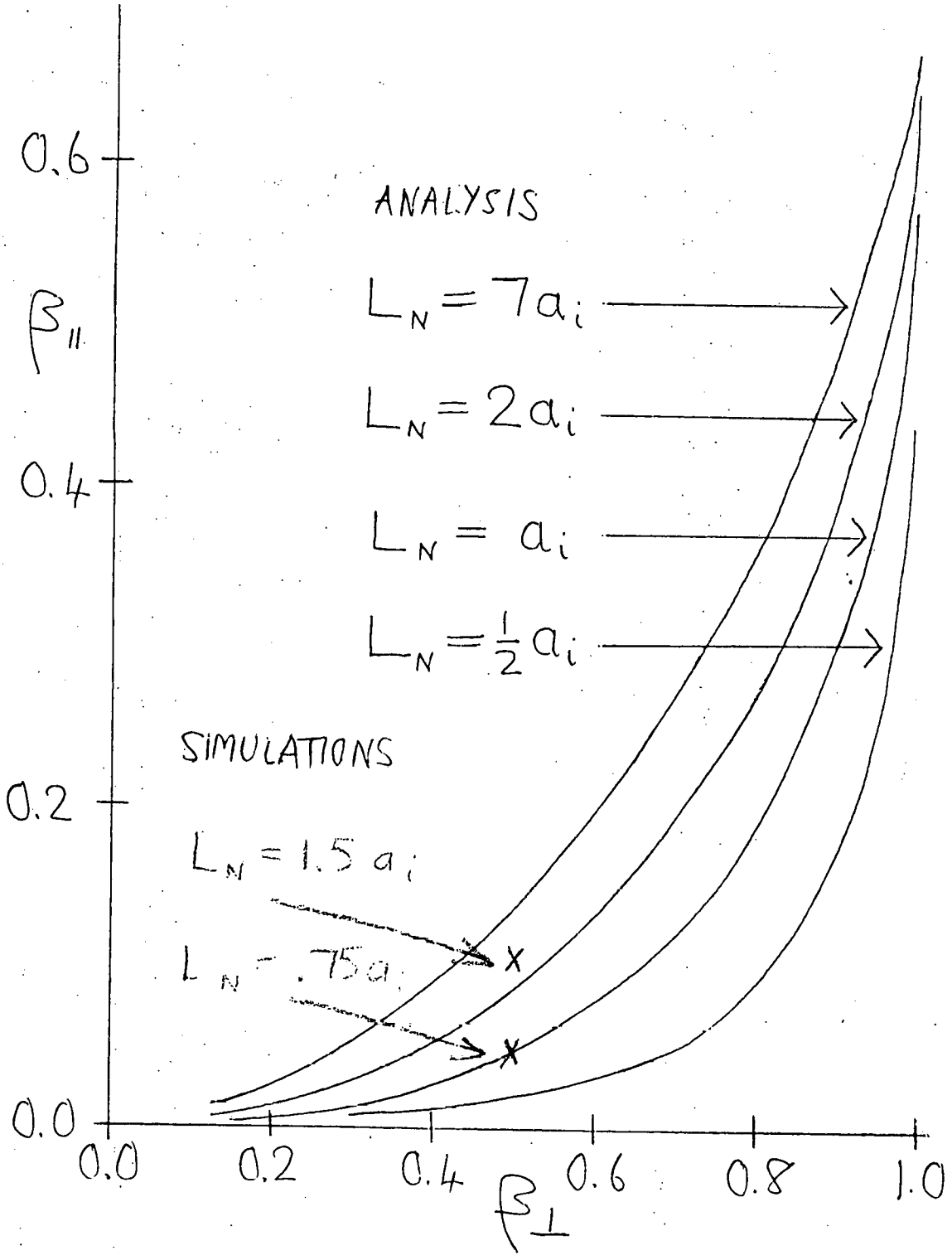

and forms of $D(\underline{K}_{\parallel}, W)$ incorporating not only non-zero $k_{\perp}^2$ but also explicit radial gradient terms. In sections V through VII various physically-motivated ion-velocity distribution-functions are described, together with the conditions for their use, the forms of D to which they give rise and the stability boundaries that result from their use. In section VIII the effect of AIC turbulence on the ion distribution function is described. The consideration of exact phase integrals and explicit gradient terms is left to a later paper.

V. Distributions of the Holdren Type

The collisional or Holdren[16] distribution is an analytic approximation to the steady-state behavior of ions dominated by ion-ion collisions and unaffected by ambipolar potential. Baldwin[18] has shown that ion-ion collisions can outpace electron drag only if

$$\frac{T_e}{T_i} \gg 0.1 \tag{38}$$

On the other hand, ambipolar potential can be neglected only if

$$\frac{T_e}{T_i} \ll 1.0 \tag{39}$$

Thus there is hardly a temperature-ratio for which the Holdren distribution is appropriate. Further, the Holdren derivation assumes a magnetic square well, whereas real mirror plasmas steepen their own wells near the machine midplane. Thus the Holdren distribution has mainly historical interest, as being an early attempt to take account of diffusion by constructing a function sloping smoothly down to a loss-boundary. The ion velocity distribution is explicitly

$$f_o(v_\perp, v_\parallel) = \frac{1}{N_{om}} \left(\frac{\alpha}{\pi}\right)^{3/2} e^{-\alpha v^2} \left(\alpha v^2\right)^m \left[\frac{R_{oc} v_\perp^2}{v^2} - 1 + \left(2R_{oc} - 3\right) \ln \frac{R_{oc} v_\perp^2}{v^2}\right] \tag{40}$$

at the center plane and

$$f(v_\perp, v_\parallel) = \frac{1}{N_{om}} \left(\frac{\alpha}{\pi}\right)^{3/2} e^{-\alpha v^2} \left(\alpha v^2\right)^m \left[\frac{R_c v_\perp^2}{v^2} - 1 + \left(2R_{oc} - 3\right) \ln \frac{R_c v_\perp^2}{v^2}\right] \tag{41}$$

at other points along the "representative" field line. In (41)

$$R_c = R_{oc} B_o/B \tag{42}$$

The distribution (40) is normalized to unity by choosing

$$N_{oo} = \left(2R_{oc} - 3\right)\left[\ln R_{oc} + 2\ln\left(1 + \sqrt{1 - R_{oc}^{-1}}\right) - 2\sqrt{1 - R_{oc}^{-1}}\right] + \frac{2}{3} R_{oc} \left(1 - R_{oc}^{-1}\right)^{3/2} \tag{43}$$

$$N_{om} = N_{oo} \cdot \left[\frac{3}{2} \cdot \frac{5}{2} \ldots \text{ to m terms}\right] \tag{44}$$

Note that the ion distribution described by (40), (41) is delimited by a loss-cone, is the product of a function of velocity only times a function of angle only, and reduces to a distribution of type (9) for the special case $m = 1$, $R_{oc} = 3/2$. For this class of distributions the relation corresponding to (22) is, for any m,

$$\frac{P_{o\parallel}}{P_o} = \frac{1}{N_{oo}} \left\{ \left(2R_{oc} - 3\right)\left[\ln R_{oc} + 2\ln\left(1 + \sqrt{1 - R_{oc}^{-1}}\right) - 2\sqrt{1 - R_{oc}^{-1}} - \frac{2}{3}\left(1 - R_{oc}^{-1}\right)^{3/2}\right] + \frac{2}{5} R_{oc}\left(1 - R_{oc}^{-1}\right)^{5/2} \right\} \tag{45}$$

On substituting (40) in (16), the AIC parallel-propagation dispersion-relation assumes the forms, valid at the midplane,

$$D(K_\parallel, W) = \frac{K_\parallel^2}{\tilde{\beta}_o} + \frac{W^2}{W-1} + \frac{1}{N_{oo}} \left\{ \left(R_{oc} - 1\right) X_o Z'\left(\xi_o\right) + \int_0^{X_o} dx\, x^2 \left[R_{oc} \frac{2W - 1}{W - 1} + \frac{2R_{oc} - 3}{1 - x^2} \frac{W}{W - 1}\right] Z'\left(\xi_o \frac{X_o}{x}\right) \right\} \quad (m = 0) \tag{46}$$

$$D(K_{\parallel}, W) = \frac{K_{\parallel}^2}{\tilde{\beta}_o} + \frac{W^2}{W-1} + \frac{1}{N_{o1}} \left\{ R_{oc} X_o^3 \left[\frac{1}{2} + \left(R_{oc} - 1\right) \frac{W}{W-1} \right] Z'(\xi_o) \right.$$

$$\left. + \left(R_{oc} - 1\right) X_o \left[\left(1 + \xi_o^2\right) Z'(\xi_o) - 1 \right] + \int_0^{X_o} dx\, x^4 \frac{2R_{oc} - 3}{(1 - x^2)^2} \frac{W}{1 - W} Z'\left(\xi_o \frac{X_o}{x}\right) \right\}$$

$$(m = 1) \qquad (47)$$

In (46) and (47) the definitions (24) are used except that now

$$\xi_o = \frac{W - 1}{X_o K_{\parallel}} \sqrt{\frac{3 + 2m}{3}} \qquad X_o = \sqrt{1 - R_{oc}^{-1}} \qquad (48)$$

The expressions (46), (47) can be used to plot convective-absolute stability boundaries in the $\beta_{\perp}$ - $\beta_{\parallel}$ plane for infinite homogeneous plasma. The resulting curves lie between the corresponding curves for the bimaxwellian and cut-maxwellian displayed in section III.

The inclusion of a non-zero $K_{\perp}$ in (46), (47) has not furnished any expression suitable for repeated computation in a reasonable time. The stabilization of the AIC mode due to finite device width has therefore not been investigated for ion distributions of the Holdren type.

The self-consistent longitudinal variation (41) of the Holdren distribution leads to the off-mid-plane AIC dispersion functions

$$D(K_{\parallel}, W) = \frac{K_{\parallel}^2}{\tilde{\beta}_o} + \frac{N_o}{N_{oo}} \frac{W^2}{\tilde{B}(W - \tilde{B})} + \frac{1}{N_{oo}} \left\{ \left(R_{oc} - 1\right) XZ'(\xi) \right.$$

$$\left. + \int_0^X dx\, x^2 \left[R_c \frac{2W - \tilde{B}}{W - \tilde{B}} + \frac{2R_{oc} - 3}{1 - x^2} \frac{W}{W - \tilde{B}} \right] Z'\left(\xi \frac{X}{x}\right) \right\} \qquad (m = 0) \qquad (49)$$

$$D(K_{\parallel}, W) = \frac{K_{\parallel}^2}{\tilde{\beta}_o} + \frac{N_1}{N_{o1}} \frac{W^2}{\tilde{B}(W - \tilde{B})} + \frac{1}{N_{o1}} \left\{ R_c X^3 \left[\frac{1}{2} + \left(R_{oc} - 1\right) \frac{W}{W - \tilde{B}} \right] Z'(\xi) \right.$$

$$\left. + \left(R_{oc} - 1\right) X \left[\left(1 + \xi^2\right) Z'(\xi) - 1 \right] + \int_0^X dx\, x^4 \frac{2R_{oc} - 3}{\left(1 - x^2\right)^2} \frac{W}{\tilde{B} - W} Z'\left(\xi \frac{X}{x}\right) \right\} \quad (m = 1) \tag{50}$$

The normalized quantities used here are those defined in (24), (31) and (42) - (44) with the addition of

$$\xi = \frac{W - \tilde{B}}{KX} \sqrt{\frac{3 + 2m}{3}} \qquad X = \sqrt{1 - R_c^{-1}} \tag{51}$$

$$N_o = \left(2R_{oc} - 3\right) \left[\ln R_c + 2 \ln \left(1 + \sqrt{1 - R_c^{-1}}\right) - 2\sqrt{1 - R_c^{-1}} \right] + \frac{2}{3} R_c \left(1 - R_c^{-1}\right)^{3/2} \tag{52}$$

$$N_m = N_o \left[\frac{3}{2} \cdot \frac{5}{2} \ldots \text{ to m terms} \right] \tag{53}$$

The expressions (49), (50) can be used to investigate finite-length stabilization of the AIC mode in 2X and MX. One makes the WKB approximation and the parabolic z-dependence approximation, so that the equation (30) is again used. The predictions for anisotropies and total betas attainable in stable operation are displayed in Figs. (12) and (13).

12

ALFVÈN-ION-CYCLOTRON MODE
(CONVECTIVE-ABSOLUTE TRANSITION)
AND MIRRORMODE CRITERION
(CENTERPLANE ONSET)
FOR HOLDREN (COLLISIONAL) DISTRIBUTION
($m = 0$)

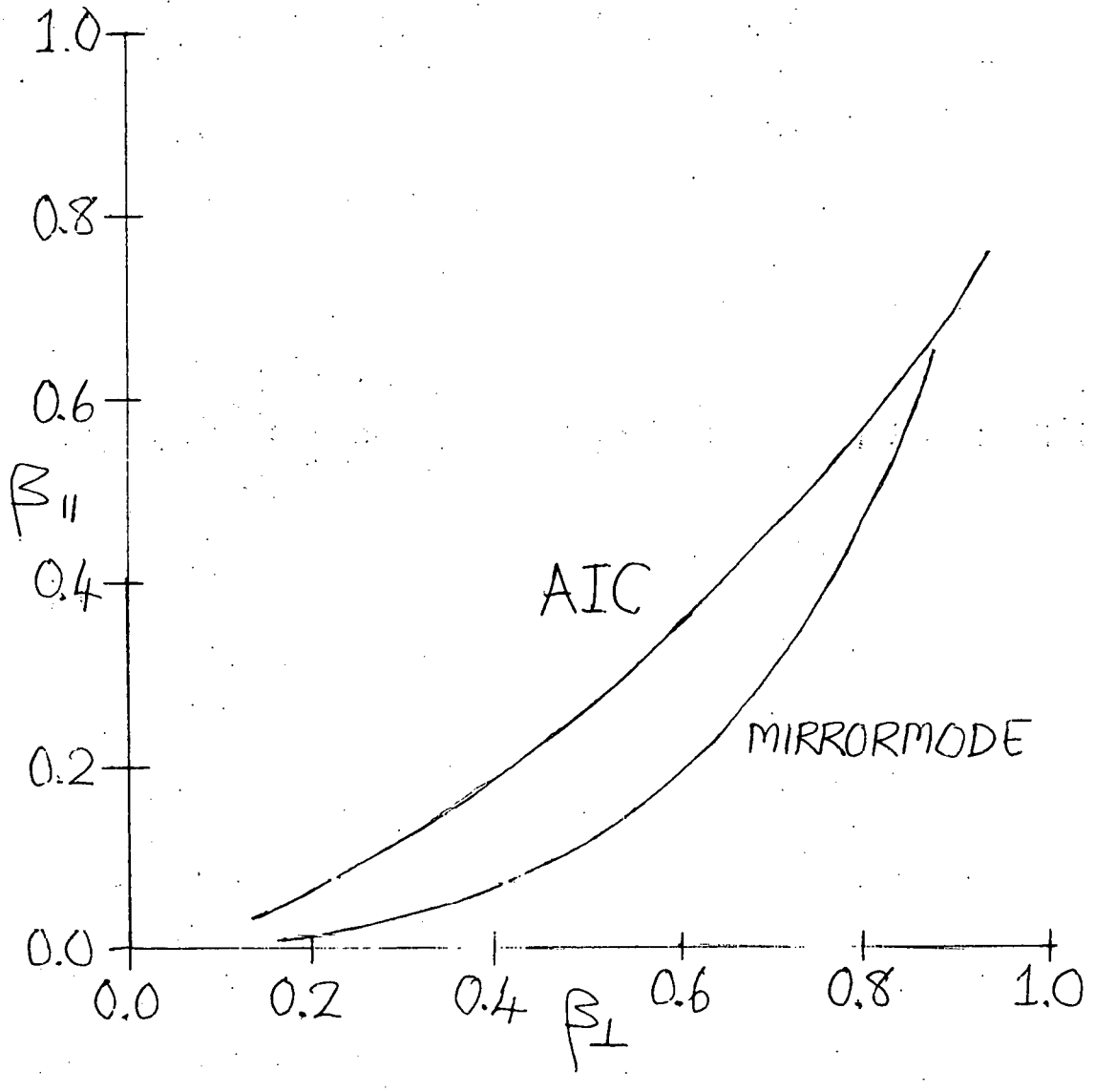

13

CONVECTIVE-ABSOLUTE BOUNDARIES FOR 2X, MX, AND INFINITE PLASMA FINITE-LENGTH EFFECTS ONLY.
HOLDREN-TYPE ION VELOCITY DISTRIBUTION
$(m = 0)$

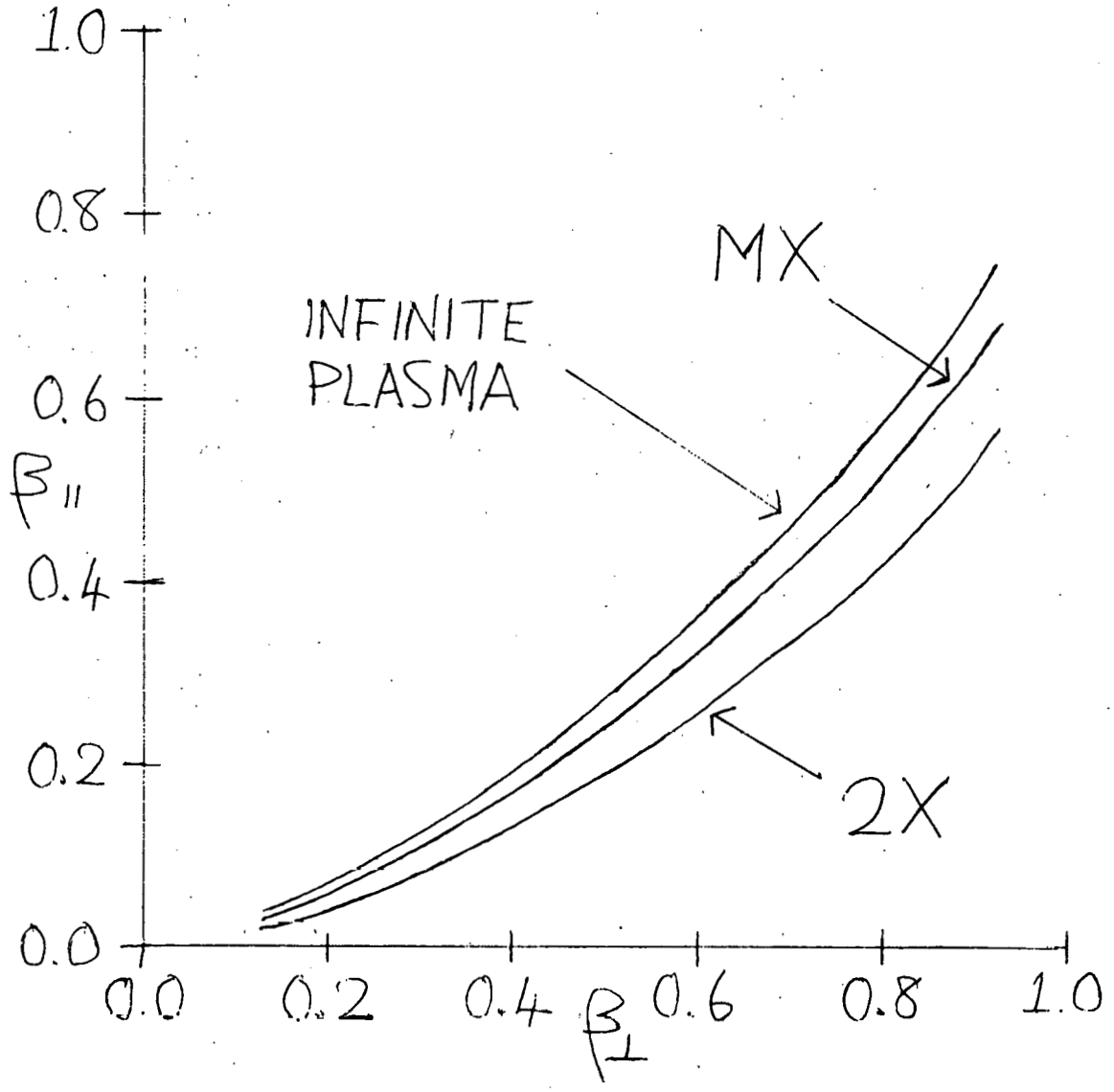

$2X: R_p = \infty \qquad L_B^{VACUUM} = 15\, a_i^{VACUUM}$

$MX: R_p = \infty \qquad L_B^{VACUUM} = 50\, a_i^{VACUUM}$

VI. Distributions Whose Angular Spread is a Function of Velocity

The class of distributions described in this section is a generalization of the "tractable" distributions discussed in section III. The underlying two-temperature maxwellian factor in the expression (9) is retained; the loss-hyperboloid factor is replaced by a factor which goes to zero on a boundary which approaches $v_{\parallel} = 0$ as v gets large:

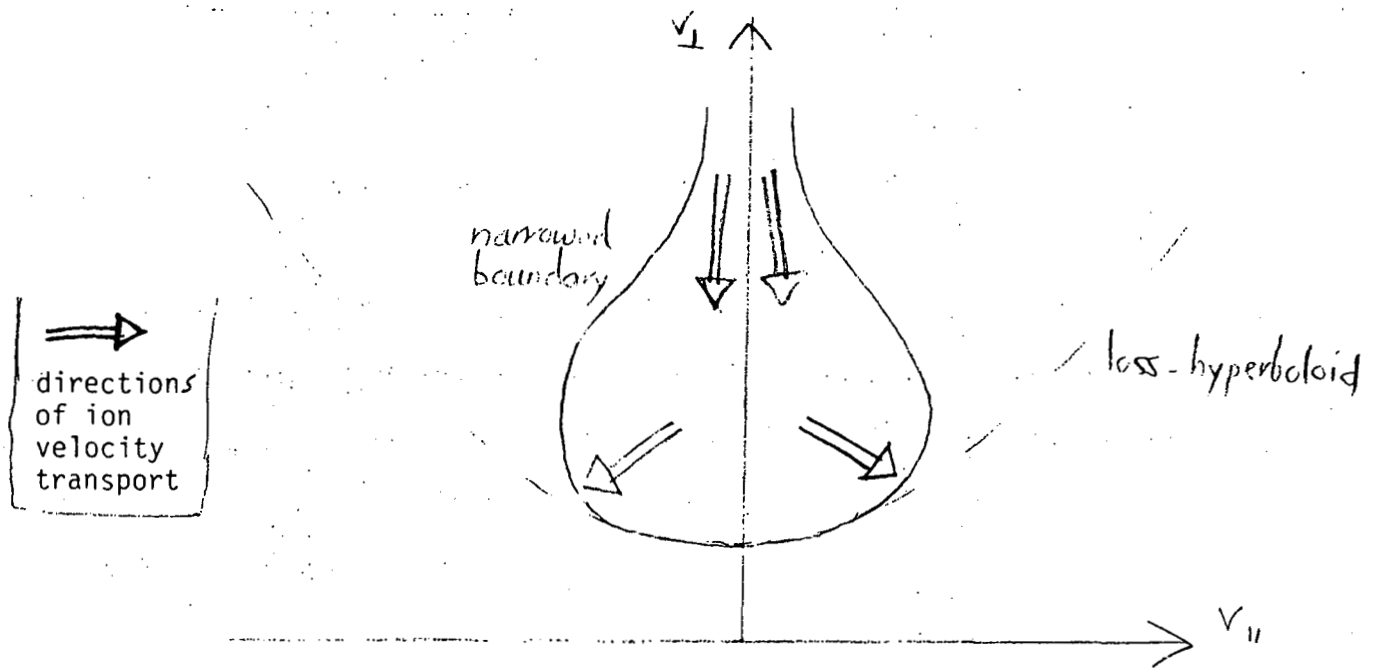

Fig. (14)

This shape of ion distribution is intended[19] to describe the plasma in a reactor, where the electrons have time to warm up to 0.1 T_i or greater. Then, as discussed by Baldwin,[18] ion-ion collisions become dominant in the main (thermal) body of the distribution, whereas electron drag remains dominant in the hot (injected) tail. Explicitly the mathematical form chosen to represent the distribution at the midplane is

$$f_o(v_\perp, v_\parallel) = \frac{1}{n!}\,\frac{\alpha_{o\perp}}{\pi}\sqrt{\frac{\alpha_{o\parallel}}{\pi} + \frac{\alpha_{o\perp}}{\pi\left(R_{oc}-1\right)}}\;\left(1 + (2n+1)\,c\right)^{n+3/2}$$

$$e^{-\alpha_{o\perp}v_\perp^2-\alpha_{o\parallel}v_\parallel^2-\alpha_{o\perp}v_h^2}\cdot\left[\left(\alpha_{o\perp}v_\perp^2 + \alpha_{o\parallel}v_\parallel^2 - \alpha_{o\perp}v_{oh}^2\right)e^{-2c\left(\alpha_{o\perp}v_\perp^2 + \alpha_{o\parallel}v_\parallel^2 - \alpha_{o\perp}v_{oh}^2\right)}\right.$$

$$\left. - \left(\alpha_{o\parallel} + \frac{\alpha_{o\perp}}{R_{oc}-1}\right)v_\parallel^2\right]^n \quad \text{when square bracket is}$$

positive, zero otherwise. (54)

Note the close resemblance between (54) and (9). Indeed (54) reduces to (9) on setting $c = 0$. The equation relating the parameters appearing in (54) to the overall pressure anisotropy is now

$$\frac{P_{o\perp}}{P_{o\parallel}} = -\frac{1}{2}\,\frac{\alpha_{o\parallel}}{\alpha_{o\perp}} + \left(\frac{\alpha_{o\parallel}}{\alpha_{o\perp}} + \frac{1}{R_{oc}-1}\right)\left[n + \frac{3}{2} + \alpha_{o\perp}v_{oh}^2\left(1 + (2n+1)\,c\right)\right]$$

$$\cdot\left(\frac{1 + (2n+3)\,c}{1 + (2n+1)\,c}\right)^{n+\frac{5}{2}} \tag{55}$$

As expected this reduces to (22) for $c = 0$. On substituting (54) in (16), the AIC parallel-propagation dispersion-function assumes the forms, valid at the midplane,

$$D(K_\parallel, W) - \frac{K^2}{\tilde{\beta}_o} + \frac{W^2}{W-1} + \frac{\eta_{oo}}{\sqrt{\pi}}\int_{-\infty}^{\infty}\frac{dt\;te^{-t^2}}{te^{-ct^2} - \xi_{oo}}\left[\left(1 - 2ct^2\right)\left(\frac{1}{1-W} - \frac{\alpha_{o\parallel}}{\alpha_{o\perp}}\right)\right.$$

$$\left.\cdot\; e^{-2ct^2} - \frac{\alpha_{o\parallel}}{\alpha_{o\perp}}\left\{\left(t^2 + h_o^2\right)\left(1 + \frac{\alpha_{o\perp}/\alpha_{o\parallel}}{R_{oc}-1}\right) - t^2e^{-2ct^2}\right\}\right]$$

$$(n = 0) \tag{56}$$

$$D(K_{\parallel}, W) = \frac{K_{\parallel}^2}{\tilde{\beta}_o} + \frac{W^2}{W-1} + \frac{\eta_{o1}}{\sqrt{\pi}} \int_{-\infty}^{\infty} \frac{dt\ t\ e^{-t^2}}{te^{-ct^2} - \xi_{o1}} \left(1 - 2ct^2\right) e^{-2ct^2}$$

$$\left[\left(\frac{1}{1-W} - \frac{\alpha_{o\parallel}}{\alpha_{o\perp}}\right)\left(\frac{1}{(1+2c)^2} + \frac{t^2}{1+2c} - t^2\right) e^{-2ct^2}\right.$$

$$\left. - \frac{\alpha_{o\parallel}}{\alpha_{o\perp}}\left[\left(1 + t^2 + h_o^2\right)\left(1 + \frac{\alpha_{o\perp}/\alpha_{o\parallel}}{R_{oc} - 1}\right) - t^2 e^{-2ct^2}\right]\right] \qquad (n = 1) \qquad (57)$$

Here the definitions (24) are used except that now

$$\xi_{on} = \frac{W-1}{K}\sqrt{\frac{\beta_o}{\beta_{o\parallel}}}\ \frac{\left(1 + (2n+1)\ c\right)^{n/2 + 3/4}}{\left(1 + (2n+3)\ c\right)^{n/2 + 5/4}}\ ;\ \eta_{on} = \frac{\left(1 + (2n+1)c\right)^{n + 3/2}}{n!} \qquad (58)$$

The contour of integration need be deformed (alternatively the pole contributions need be explicitly added) only if the real phase velocity lies within the ion distribution <u>and</u> the imaginary part of the phase velocity is less than zero. More explicitly, the combination of the conditions

$$|\mathrm{Re}\left(\xi_o\right)| < \frac{1}{\sqrt{2c}} \qquad \mathrm{Im}\left(\xi_o\right) < 0$$

requires that the integration contour in the t-plane be deformed as follows; remember that $\mathrm{Re}\left(\xi_o\right)$ is negative;

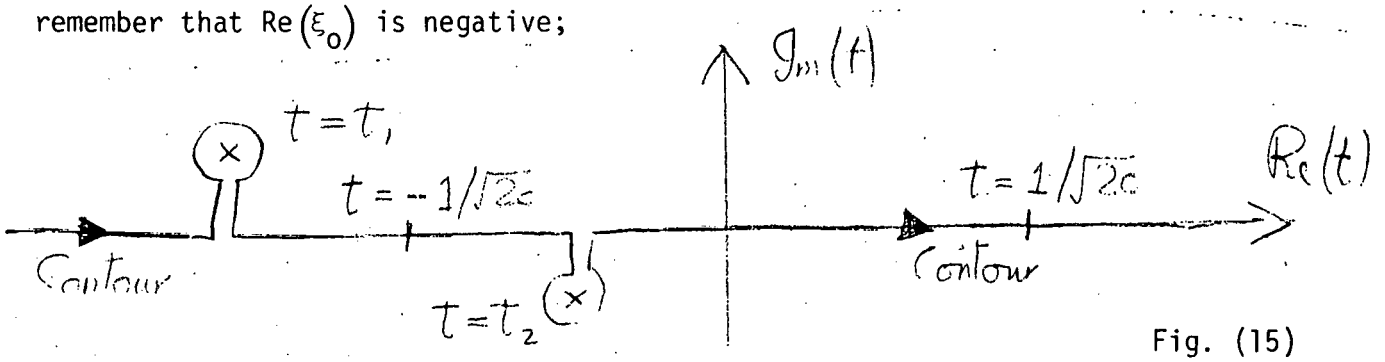

Fig. (15)

In the above diagram t_1 and t_2 are the roots of $te^{-ct^2} = \xi_o$.

The expressions (56), (57) can be used to plot convective-absolute stability boundaries in the $\beta_\perp - \beta_\parallel$ plane for infinite homogeneous plasma.

Fix all but one of the free parameters appearing on the right-hand side of (55). The most straightforward choice is the choice which isolates the effect of the boundary-narrowing illustrated in Fig. (14). This choice is

$$n = 0;\ v_{oh} = 0;\ R_{oc} = \infty;\ \alpha_{o\perp}/\alpha_{o\parallel} = 1 \tag{59}$$

The remaining parameter c then describes the rapidity of onset of that boundary-narrowing. Spot checks on these boundaries yield points lying between the corresponding curves for the bimaxwellian and cut-maxwellian displayed in section III.

The inclusion of a non-zero $K_\perp$ in (56), (57) has not furnished any expression suitable for repeated computation in a reasonable time. The stabilization of the AIC mode due to finite device width has therefore not been investigated.

The self-consistent longitudinal variation of the distribution (54) with increasing magnetic field leads to a finite cutoff in $v_\perp$. Thus there is a qualitative difference between the form of the ion velocity distribution at the midplane and the form of the distribution away from the midplane. This is a physically unsatisfying feature of the form (54).

Explicitly the distribution function off the midplane is

$$f(v_\perp, v_\parallel) = \frac{1}{n!}\ \frac{\alpha_{o\perp}}{\pi}\sqrt{\frac{\alpha_{o\parallel}}{\pi} + \frac{\alpha_{o\perp}}{\pi\left(R_{oc} - 1\right)}}\ \left(1 + (2n+1)c\right)^{n + 3/2}\ e^{-g}$$

$$\left[ge^{-2cg} - \left(\alpha_{o\parallel} + \frac{\alpha_{o\perp}}{R_{oc} - 1}\right)\left(v_\parallel^2 + \frac{B - B_o}{B}\ v_\perp^2 - 2\left(\phi_o - \phi\right)\right)\right]^n \tag{60}$$

when square bracket is positive, zero otherwise. Here one uses (11) with the

addition of

$$g \equiv \alpha_\perp v_\perp^2 + \alpha_\parallel v_\parallel^2 - \alpha_{o\perp} v_{oh}^2 - 2\alpha_\parallel \left(\phi_o - \phi\right) \tag{61}$$

The functional form of the distribution is qualitatively different away from the midplane. One cannot express (60) as a multiple of the function (54) with appropriately adjusted parameters, as (10) was expressed in terms of (9). However some simplification occurs on taking a linear dependence of potential on B as in (12), chosen to yield perfect confinement for the tractable distribution (10). In other words, assume

$$2\left(\phi_o - \phi\right) = \frac{\left(B - B_o\right)}{B_o} v_{oh}^2 = \frac{\left(B - B_o\right)}{B} v_h^2 \tag{62}$$

then (60) becomes

$$f(v_\perp, v_\parallel) = \frac{1}{n!} \frac{\alpha_{o\perp}}{\pi} \sqrt{\frac{\alpha_{o\parallel}}{\pi} + \frac{\alpha_{o\perp}}{\pi\left(R_{oc} - 1\right)}} \left(1 + (2n + 1)\, c\right)^{n + 3/2}$$

$$e^{-\alpha_\perp v_\perp^2 - \alpha_\parallel v_\parallel^2 + \alpha_\perp v_h^2} \left[\left(\alpha_\perp v_\perp^2 + \alpha_\parallel v_\parallel^2 - \alpha_\perp v_h^2\right) e^{-2c\left(\alpha_\perp v_\perp^2 + \alpha_\parallel v_\parallel^2 - \alpha_\perp v_h^2\right)} - \left(\alpha_{o\parallel} + \frac{\alpha_{o\perp}}{R_{oc} - 1}\right) \left(v_\parallel^2 + \frac{B - B_o}{B} \left(v_\perp^2 - v_h^2\right)\right) \right]^n \tag{63}$$

This form of variation along field lines will be used to estimate the finite-length stabilization of the AIC mode.

On substituting (63) into (16), the AIC parallel-propagation dispersion function assumes the forms, valid away from the midplane,

$$D(K_{\parallel}, W) = \frac{K_{\parallel}^2}{\tilde{\beta}_o} + \frac{W^2 N_o}{\tilde{B}(W - \tilde{B})} + \frac{\eta_o}{\sqrt{\pi}} \int_{-T}^{T} \frac{dt\ t\ e^{-t^2}}{t\sqrt{\frac{e^{-2ct^2} - G}{1 - G}} - \xi_o}$$

$$\left\{ \left(\frac{\tilde{B}}{\tilde{B} - W} - \frac{\alpha_{\parallel}}{\alpha_{\perp}} \right) \left(\frac{(1 - 2ct^2)e^{-2ct^2} - G}{1 - G} \right) - \frac{\alpha_{\parallel}}{\alpha_{\perp}} \left[\left(t^2 + h^2\right)\left(1 + \frac{\alpha_{\perp}/\alpha_{\parallel}}{R_c - 1}\right) - t^2 \left(\frac{e^{-2ct^2} - G}{1 - G} \right) \right] \right\} \qquad (n = 0) \quad (64)$$

$$D(K_{\parallel}, W) = \frac{K_{\parallel}^2}{\tilde{\beta}_o} + \frac{W^2 N_1}{\tilde{B}(W - \tilde{B})} + \frac{\eta_1}{\sqrt{\pi}} \int_{-T}^{T} \frac{dt\ t\ e^{-t^2}\left(e^{-2ct^2}(1 - 2ct^2) - G\right)}{\left[t\sqrt{\frac{e^{-2ct^2} - G}{1 - G}} - \xi_1\right][1 - G]}$$

$$\left\{ \left(\frac{\tilde{B}}{\tilde{B} - W} - \frac{\alpha_{\parallel}}{\alpha_{\perp}} \right) \left[\frac{e^{-2ct^2}\left(1 + (1 + 2c)t^2\right)/(1 + 2c)^2 - t^2 e^{-2ct^2} - G}{1 - G} \right] - \frac{\alpha_{\parallel}}{\alpha_{\perp}} \left[\left(1 + t^2 + h^2\right)\left(1 + \frac{\alpha_{\perp}/\alpha_{\parallel}}{R_c - 1}\right) - \frac{t^2\left(e^{-2ct^2} - G\right)}{1 - G} \right] \right\} \qquad (n = 1) \quad (65)$$

Here the definitions (11), (24), (31), (58) are used except that now

$$\xi_n = \frac{W - B}{K} \sqrt{\frac{\beta_o}{\beta_{o\parallel}}} \frac{\left(1 + (2n + 1)c\right)^{n/2 + 3/4}}{\left(1 + (2n + 3)c\right)^{n/2 + 5/4}} \sqrt{\frac{R_{oc} - 1}{R_{oc} - \tilde{B}}}$$

$$\eta_n = \frac{\left(1 + (2n + 1)c\right)^{n + 3/2}}{n!} \left(\frac{\alpha_{o\perp}}{\alpha_{\perp}}\right)^{n + 1} \tilde{B}^{1/2} \left(\frac{R_c - 1}{R_{oc} - 1}\right)^{n + 1/2}$$

$$G = 1 - \frac{\alpha_{o\perp}}{\alpha_{\perp}} \left(\frac{R_c - 1}{R_{oc} - 1}\right) \qquad T^2 = \frac{\ln C}{2c} \qquad (66)$$

$$N_o = \frac{\eta_o}{\sqrt{\pi}} \int_o^{T^2} dt^2 e^{-t^2} \frac{\dfrac{\left(e^{-2ct^2}\left(1 - 2ct^2\right) - G\right)}{1 - G}}{t\sqrt{\dfrac{e^{-2ct^2} - G}{1 - G}}} \tag{67}$$

$$N_1 = \frac{\eta_1}{\sqrt{\pi}} \int_o^{T^2} dt^2 e^{-t^2} \frac{\dfrac{\left(e^{-2ct^2}\left(1 - 2ct^2\right) - G\right)}{1 - G}}{t\sqrt{\dfrac{e^{-2ct^2} - G}{1 - G}}}$$

$$\left[\frac{e^{-2ct^2}\left(1 + (1 + 2c)t^2\right)/(1 + 2c)^2 - t^2 e^{-2ct^2} - G}{1 - G} \right] \tag{68}$$

The factors of $(1 - G)$ in the denominators of (64), (65) are placed so as to facilitate comparison with the dispersion functions (23), (33), to which (64), (65) reduce for $c = 0$. The factors of $(1 - G)$ in (67), (68) facilitate comparison with the coefficient of F in (10), which constitutes the density relative to the midplane density.

The expressions (64), (65) can be used to investigate finite-length stabilization of the AIC mode in 2X and MX. Make the WKB approximation and the parabolic z-dependence approximation so that equation (30) is again used. This work has not been done by us yet.

VII. Numerically Specified Distributions

There exist computer codes[14] which follow the evolution of ion velocity distributions under the combined influence of electron drag, ion-ion collisions and drift-cyclotron-loss-cone turbulence. These codes reach a steady state. The ion velocity distribution in this steady state is the numerically specified distribution referred to above. This distribution will vary from run to run, affording a way to cover the $\beta_\perp - \beta_\parallel$ plane. However this covering is not unique, since (as with the distributions described in sections IV, V, VI) a given point in the $\beta_\perp - \beta_\parallel$ plane can be reached in more than one way -- in this case, by more than one set of starting conditions for the computer code. Nevertheless, a scattering of discrete points in the $\beta_\perp - \beta_\parallel$ plane, each with AIC stability information attached, is expected to be a useful adjunct to the continuous stability boundaries drawn earlier for analytic distributions.

The discussion of this section does not include the effect of the AIC activity on the distribution function. The self-consistent treatment of AIC turbulence, ion velocity-space diffusion, AIC stabilization, and final AIC-compatible distributions is outlined in Section VIII.

The Fokker-Planck code[14] furnishes an ion velocity distribution, specified up to the parallel distribution of the first few perpendicular moments. Let $\alpha_\perp$, $\alpha_\parallel$ be any conveniently chosen inverse scale temperatures, then the code furnishes a midplane distribution

$$G_p(u_\parallel) = \int_0^\infty du_\perp^2 \, u_\perp^{2p} \, F_0(u_\parallel, u_\perp) \qquad p = 0, 1, 2 \tag{69}$$

with

$$u_{\parallel} = v_{\parallel}\sqrt{\alpha_{\parallel}} \qquad u_{\perp} = v_{\perp}\sqrt{\alpha_{\perp}} \qquad F_0 = \frac{\pi}{\alpha_{\perp}}\sqrt{\frac{\pi}{\alpha_{\parallel}}}\, f_0$$

$$1 \equiv \int d^3v f_0 = \frac{1}{\sqrt{\pi}} \int_{-\infty}^{\infty} du_{\parallel} \int_0^{\infty} du_{\perp}^2\, F_0 = \frac{1}{\sqrt{\pi}} \int_{-\infty}^{\infty} du_{\parallel}\, G_0 \tag{70}$$

This is an adequate description of the ion velocity distribution as far as the parallel-propagating AIC mode is concerned. Substituting (69) in (16) one obtains the form, valid at the midplane,

$$D(K_{\parallel}, W) = \frac{K^2}{\tilde{\beta}_0} + \frac{W^2}{W-1} + \frac{1}{\sqrt{\pi}} \int_{-\infty}^{\infty} \frac{du_{\parallel}\, u_{\parallel}}{u_{\parallel} - \xi_0} \left[\frac{1}{1-W}\, G_0 + \frac{\alpha_{\parallel}}{\alpha_{\perp}} \frac{dG_1}{du_{\parallel}^2}\right] \tag{71}$$

Here the normalized quantities are those of (24) and (70) except that now

$$\xi_0 = \frac{W-1}{K}\sqrt{\frac{\alpha_{\parallel}}{\alpha_{phys}}} \qquad \frac{3}{2} \equiv \langle \alpha_{phys}\, v^2 \rangle \equiv \int d^3v v^2 f_0$$

$$= \frac{1}{\sqrt{\pi}} \int_{-\infty}^{\infty} du_{\parallel} \left[\frac{\alpha_{phys}}{\alpha_{\perp}}\, G_1 + \frac{\alpha_{phys}}{\alpha_{\parallel}}\, u_{\parallel}^2\, G_0\right] \tag{72}$$

When evaluating D it is necessary to deform the contour of integration (alternatively, to include the pole contribution explicitly) if the real part of the phase velocity lies within the ion distribution and the imaginary part is negative. This occurs in all physically meaningful cases.

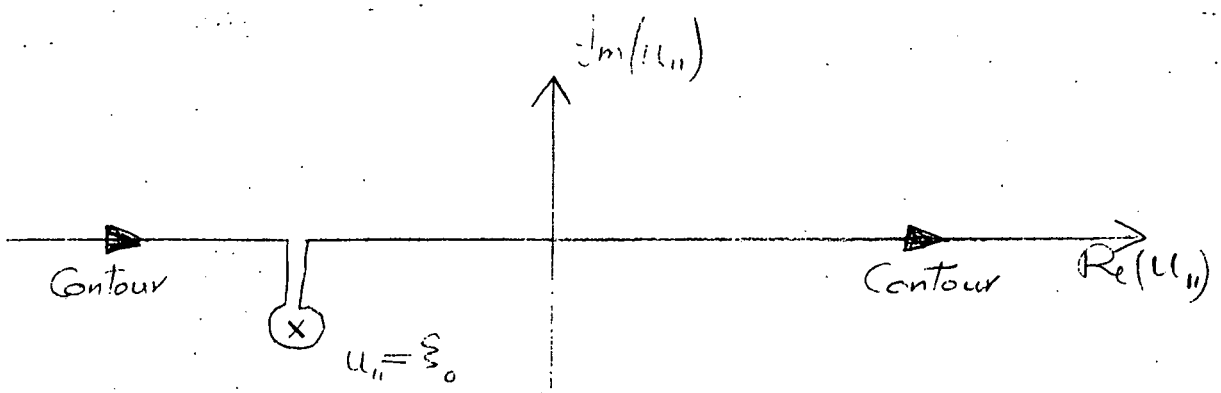

Fig. (16)

This requires extending the function enclosed in square brackets in (71) into the complex plane. To do so requires that G_0 and G_1 be expressed in terms of some basis of analytic functions. We choose the basis to be a series of parallel-velocity Maxwellians of decreasing temperature. Then the dispersion function (71) becomes the sum of a series of Z'-functions of increasing argument, with coefficients that do not depend on $K_{\parallel}$, W.

Represent the function G_p as a sum of odd Legendre polynomials in the parallel energy:

$$G_p(u_{\parallel}) = \sum_{m=0}^{\infty} b^{(p)}_{2m+1} P_{2m+1}\left(e^{-cu_{\parallel}^2}\right) \tag{73}$$

Some experience and judgement goes into choosing the scale factor c; as yet we have no rigorous way of doing it. Use the fact that the odd Legendre polynomials form an orthogonal basis on the interval (0, 1) to determine the coefficients

$$b^{(p)}_{2m+1} = \frac{1}{2(2m+1)+1} \int_0^1 d\left(e^{-cu_{\parallel}^2}\right) P_{2m+1}\left(e^{-cu_{\parallel}^2}\right) G_p(u_{\parallel}) \tag{74}$$

For purposes of carrying out this integral, take the data points specifying G_p and interpolate linearly in the space of the variable of integration

$$e^{-cu_{\parallel}^2} = x \quad \text{say} \tag{75}$$

Now transform linearly to a basis of Maxwellians. For known a_{mp},

$$p_{2m+1}\left(e^{-cu_{\parallel}^2}\right) \equiv e^{-cu_{\parallel}^2} \sum_{j=0}^{m} a_{mj}\, e^{-2jcu_{\parallel}^2} \tag{76}$$

$$\therefore \quad G_p(u_{\parallel}) = e^{-cu_{\parallel}^2} \sum_{p=0}^{\infty} A_j^{(p)}\, e^{-2jcu_{\parallel}^2} \tag{77}$$

where $\quad A_j^{(p)} = \sum_{m=j}^{\infty} b_m^{(p)}\, a_{mj}$.

$$\therefore \quad D(K_{\parallel}, W) = \frac{K^2}{\tilde{\beta}_o} + \frac{W^2}{W-1} - \frac{1}{2} \sum_{j=1}^{\infty} Z'\left(\xi_o(2j+1)c\right)$$

$$\left[\frac{A_j^{(o)}}{\sqrt{(2j+1)c}} \; \frac{1}{1-W} - A_j^{(1)} \sqrt{(2j+1)c} \; \frac{\alpha_{\parallel}}{\alpha_{\perp}} \right] \tag{78}$$

The expression (78) will be used to obtain numerous discrete points in the $\beta_{\perp} - \beta_{\parallel}$ plane, each with AIC stability information attached, as previously discussed. Of course the sum over j will be truncated using the resultant error in D as a guide.

The specification of the midplane velocity distribution by the moments (69) does not provide enough information to construct the AIC parallel-propagation dispersion function at a finite distance away from the midplane. Thus the quantity $D_{\tilde{\beta}}$ in equation (30) cannot be computed as a numerical derivative. However the moments (69) contain enough information to calculate the derivative

$D_{\tilde{B}}$ directly:

$$\frac{\partial D}{\partial \tilde{B}} = - \frac{\partial D}{\partial W} - 2W - \frac{2K^2}{\tilde{\beta}_o} + \frac{W^2}{W - 1} \frac{1}{\sqrt{\pi}} \int_{-\infty}^{\infty} du_{\parallel} \left[\frac{d2\alpha_{\parallel}\phi}{d\tilde{B}} \frac{dG_o}{du_{\parallel}^2} + \frac{\alpha_{\parallel}}{\alpha_{\perp}} \frac{dG_1}{du_{\parallel}^2} \right]$$

$$+ \frac{1}{\sqrt{\pi}} \int_{-\infty}^{\infty} \frac{du_{\parallel} u_{\parallel}}{u_{\parallel} - \xi_o} \left\{ \frac{1}{1 - W} \left[\frac{d2\alpha_{\parallel}\phi}{d\tilde{B}} \frac{dG_o}{du_{\parallel}^2} + \frac{\alpha_{\parallel}}{\alpha_{\perp}} \frac{dG_1}{du_{\parallel}^2} \right] \right.$$

$$\left. + \frac{\alpha_{\parallel}}{\alpha_{\perp}} \left[\frac{d2\alpha_{\parallel}\phi}{d\tilde{B}} \frac{d^2G_1}{du_{\parallel}^4} + \frac{\alpha_{\parallel}}{\alpha_{\perp}} \frac{d^2G_2}{du_{\parallel}^4} \right] \right\} \tag{79}$$

The ambipolar potential is provided along with the ion distribution as output of the Fokker-Planck code. In terms of the many-temperature Maxwellian decomposition (77), one has

$$\frac{\partial D}{\partial \tilde{B}} = - \frac{\partial D}{\partial W} - 2W - \frac{2K^2}{\tilde{\beta}_o} + \frac{W^2}{W - 1} \sum_{j = 1}^{\infty} \sqrt{(2j + 1)c} \left[\frac{d2\alpha_{\parallel}\phi}{d\tilde{B}} A_j^{(o)} + \frac{\alpha_{\parallel}}{\alpha_{\perp}} A_j^{(1)} \right]$$

$$+ \frac{1}{2} \sum_{j = 1}^{\infty} Z'\left(\xi_o(2j + 1)c\right) \left\{ \frac{1}{1 - W} \sqrt{(2j + 1)c} \left[\frac{d2\alpha_{\parallel}\phi}{d\tilde{B}} A_j^{(o)} + \frac{\alpha_{\parallel}}{\alpha_{\perp}} A_j^{(1)} \right] \right.$$

$$\left. - \frac{\alpha_{\parallel}}{\alpha_{\perp}} \left((2j + 1)c\right)^{3/2} \left[\frac{d2\alpha_{\parallel}\phi}{d\tilde{B}} A_j^{(1)} + \frac{\alpha_{\parallel}}{\alpha_{\perp}} A_j^{(2)} \right] \right\} \tag{80}$$

This will allow the WKB frequency shift to be estimated for the same points in the $\beta_{\perp} - \beta_{\parallel}$ plane as were taken in (78). Those points will thus have attached to them AIC stability information pertinent to 2X and MX.

VIII. Diffusion and Stabilization

The preceding seven sections have dealt with the linear stability of the Alfvén-ion-cyclotron mode. It is seen that simple models of mirror plasmas predict absolute instability at discouragingly small anisotropies like 5:1 whereas real mirror machines like 2X function happily at anisotropies estimated to run as high as 50:1. It is tempting to try and explain this by saying that nonlinear effects flatten out the distribution in the resonant region in such a way as to reconcile a zero wave growth rate with a low particle loss rate. Such a self-consistent steady-state occurs in the case of drift-cyclotron-loss-cone turbulence. In the case of AIC turbulence the 3-dimensional nature of the mode makes such a steady-state harder to attain.

Consider a model of AIC turbulence in which the power spectrum in k-space consists of a line-density distribution along the k_z-axis. Each component mode of this distribution causes diffusion in velocity space, located on the plane of ions resonant with that mode and directed along arcs of circles centered on the phase velocity of that mode[20]. The following diagram illustrates this for positive ω and positive $k_{\parallel}$.

Fig. (17)

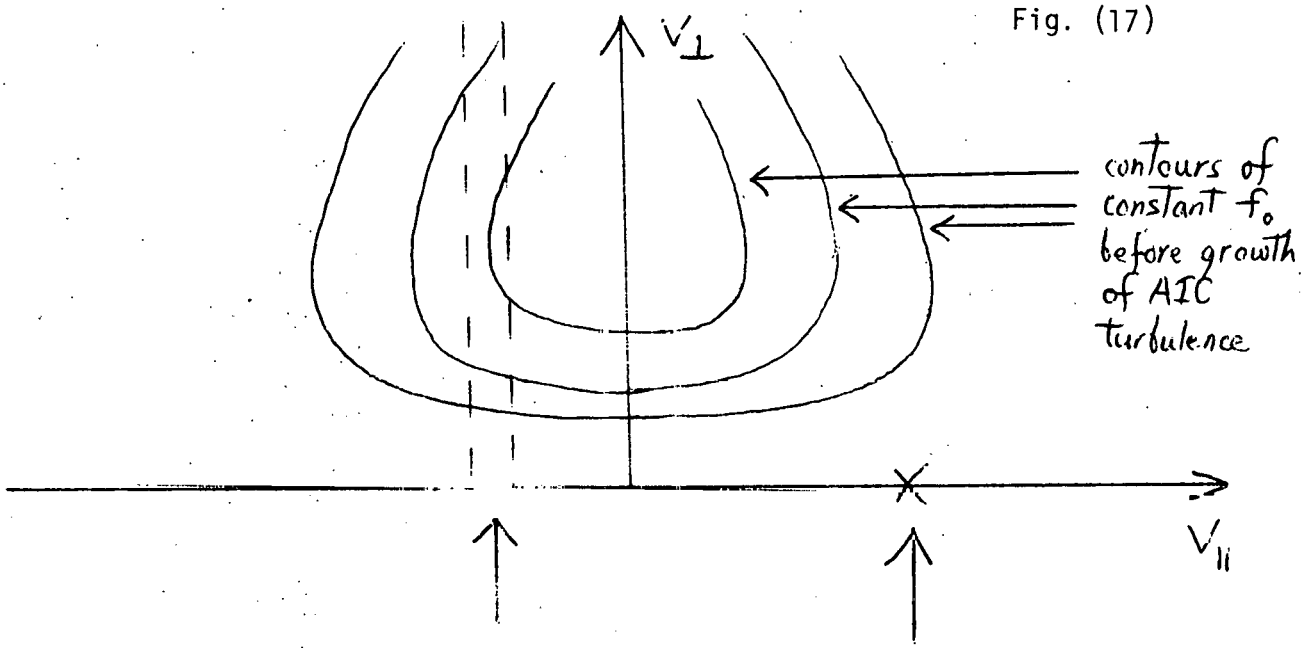

resonant region for ions

$$v_\parallel = v_{res}(k_\parallel) < 0$$

$$= \frac{\omega(k_\parallel) - \omega_{ci}}{k_\parallel}$$

phase velocity

$$v_\parallel = v_{ph}(k_\parallel) > 0$$

$$= \frac{\omega(k_\parallel)}{k_\parallel}$$

The parallel-propagation dispersion-diagram for AIC waves yields phase-velocities and resonant ion velocities that both decrease in magnitude as $k_\parallel$ increases.

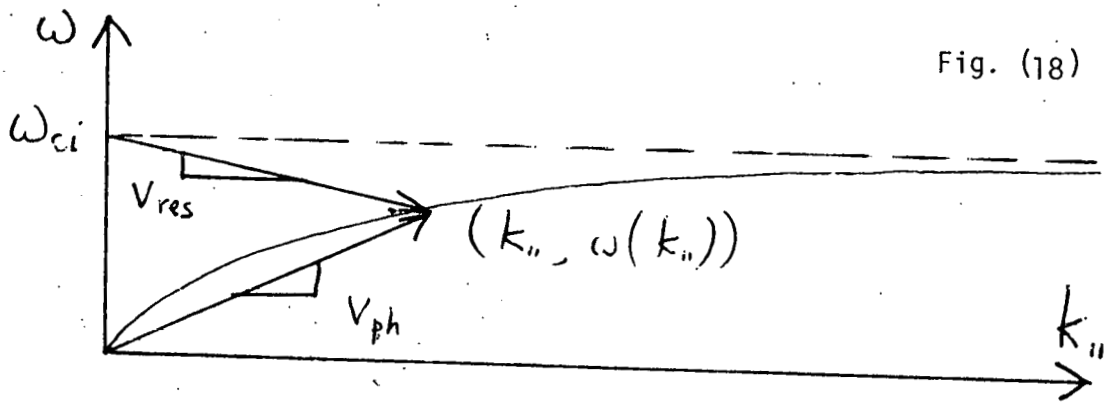

Fig. (18)

The appearance of Fig. (18) after putting in a distribution of AIC turbulence in $k_{\parallel}$ is somewhat as follows:

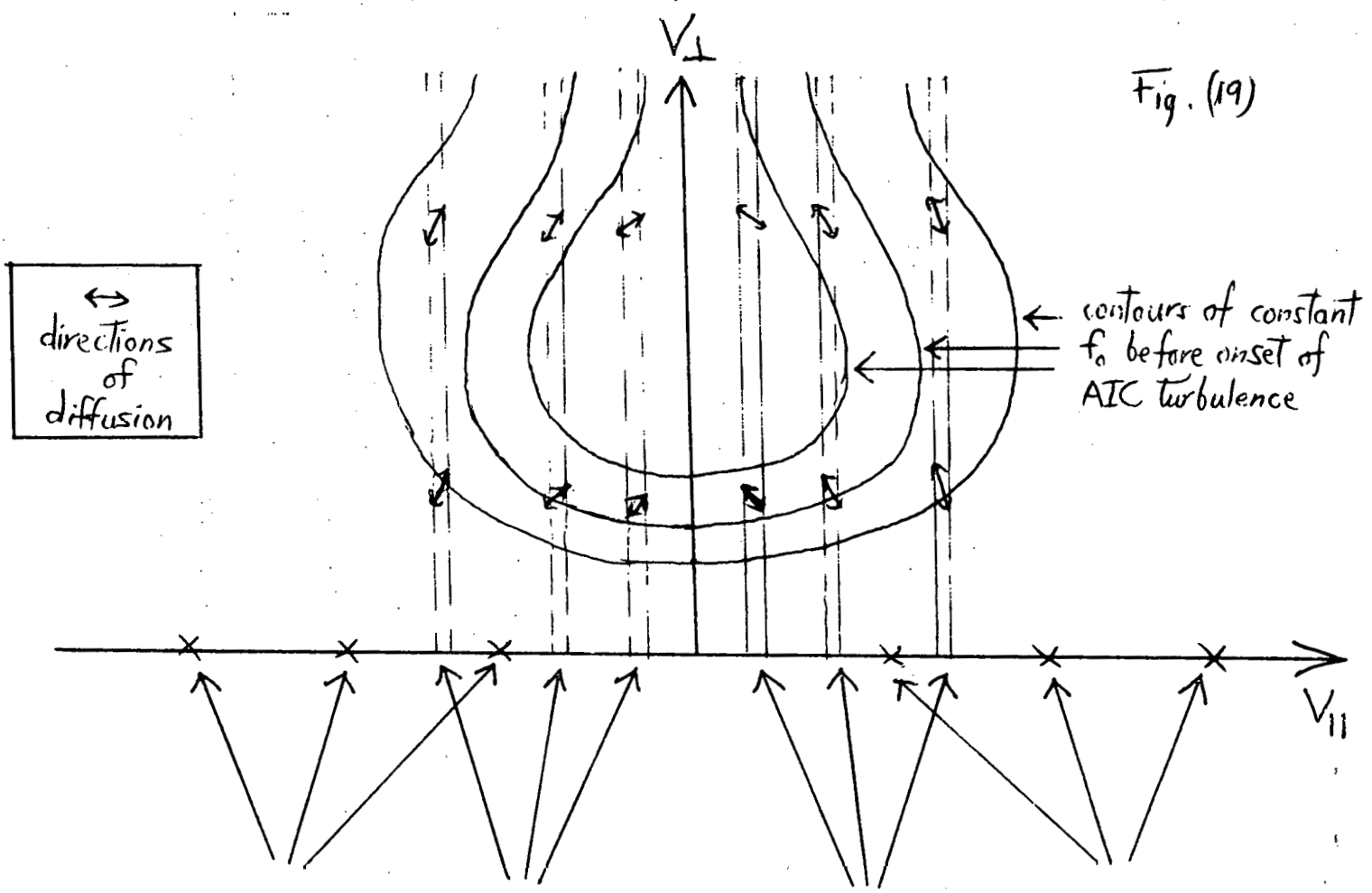

Fig. (19)

phase-velocities for negative $k_{\parallel}$ | resonant ion velocities for positive $k_{\parallel}$ | resonant ion velocities for negative $k_{\parallel}$ | phase-velocities for positive $k_{\parallel}$

We adopt the convention that ω has a positive, real part. Then the equation describing the process illustrated in Fig. (19) is[20], according to quasilinear theory,

$$\frac{\partial\langle f\rangle}{\partial t} = \frac{\pi}{2}\frac{q^2}{m^2}\int_{0<\mathrm{Re}(\omega)} dk_{\parallel}\left[\frac{\omega - k_{\parallel}v_{\parallel}}{\omega}\frac{1}{v_{\perp}}\frac{\partial}{\partial v_{\perp}}v_{\perp} + \frac{k_{\parallel}v_{\perp}}{\omega}\frac{\partial}{\partial v_{\perp}}\right]$$

$$\delta\left(k_{\parallel}v_{\parallel} + \omega_{ci} - \omega\right)\ \varepsilon(k_{\parallel})\left[\frac{\omega - k_{\parallel}v_{\parallel}}{\omega}\frac{\partial}{\partial v_{\perp}} + \frac{k_{\parallel}v_{\perp}}{\omega}\frac{\partial}{\partial v_{\perp}}\right]\langle f\rangle \tag{81}$$

$$= \int dk\ \frac{\partial}{\partial\vec{v}}\cdot\overleftrightarrow{D}_k\cdot\frac{\partial}{\partial\vec{v}}\langle f\rangle \quad \text{say} \tag{82}$$

Here the spatial spectral energy density $\varepsilon\ (k_{\parallel})$ is defined to be the mean square electric field in a unit wavevector interval.

$$\varepsilon(k_{\parallel}) \equiv \Delta\langle E_{\odot}{}^2\rangle/\Delta k_{\parallel} \tag{83}$$

Carrying out the integral over $k_{\parallel}$

$$\frac{\partial\langle f\rangle}{\partial t} = \frac{\pi}{2}\frac{q^2}{m^2}\left(\frac{1}{v_{\perp}}\frac{\partial}{\partial v_{\perp}}v_{\perp},\ \frac{\partial}{\partial v_{\parallel}}\right)\cdot\left(\frac{\omega_{ci}}{\omega},\ \frac{k_{\parallel}v_{\perp}}{\omega}\right)\left[\varepsilon\left(\omega_{ci}\right)\right]_{v_{\parallel}}$$

$$\left(\frac{\omega_{ci}}{\omega},\ \frac{k_{\parallel}v_{\perp}}{\omega}\right)\cdot\left(\frac{\partial}{\partial v_{\perp}},\ \frac{\partial}{\partial v_{\parallel}}\right)\langle f\rangle \tag{84}$$

$$= \frac{\partial}{\partial\vec{v}}\cdot\overleftrightarrow{D}\cdot\frac{\partial}{\partial\vec{v}}\langle f\rangle \text{ say} \tag{85}$$

Here $k_{\parallel} = k_{\parallel}(v)$ and $\omega = \omega(v)$ are fixed by the requirements $D(k_{\parallel}, \omega) = 0$, $k_{\parallel}v_{\parallel} - \omega + \omega_{ci} = 0$.

Here the temporal spectral energy density $\left[\varepsilon(\omega)\right]_0$ is defined to be the mean square electric field lying in a unit frequency interval, as measured in the laboratory frame

$$\left[\varepsilon(\omega')\right]_0 \equiv \Delta\langle E^2\rangle / \Delta\omega \qquad \omega = \omega' \tag{87}$$

The temporal spectral energy density $\varepsilon(\omega)_{v_{\parallel}}$ is the same quantity measured in a frame moving with parallel velocity $v_{\parallel}$. It is the mean square electric field lying in a unit interval of Doppler-shifted frequency

$$\left[\varepsilon(\omega')\right]_{v_{\parallel}} \equiv \Delta\langle E^2\rangle / \Delta(\omega - k_{\parallel}v_{\parallel}) \qquad \omega - k_{\parallel}v_{\parallel} = \omega'$$

$$= \frac{\Delta\langle E_{\Theta}{}^2\rangle / \Delta k_{\parallel}}{|\Delta(\omega - k_{\parallel}v_{\parallel}) / k_{\parallel}|} = \frac{\varepsilon(k_{\parallel})}{|v_{group} - v_{\parallel}|} \tag{88}$$

The spectral density appearing in (83) is thus just the energy density of the temporal process experienced by a particle moving with parallel velocity $v_{\parallel}$, evaluated at the resonant frequency ω_{ci}. This is what one would expect physically.

If the AIC turbulence is strong enough (just how strong will emerge from the calculation) resonance broadening[21] will take place and the δ-function of (81) must be replaced by

$$\hat{\delta}(k_{\parallel}v_{\parallel} + \omega_{ci} - \omega) = \frac{1}{\pi}\,\mathrm{Re}\int_{-\infty}^{0} dt\; e^{\,i(k_{\parallel}v_{\parallel} + \omega_{ci} - \omega)t + \omega^3 t^3} \tag{89}$$

where the broadening is given by

$$\hat{\omega}^3 = \frac{1}{3}\,\vec{k}\cdot\vec{\vec{D}}\cdot\vec{k} \tag{90}$$

and $\vec{\vec{D}}$ is given by integrating (81) over $k_{\parallel}$ with the broadened $\hat{\delta}$-function. Of course, this procedure is circular. We break the circle by starting with δ-function in (81), integrating over $k_{\parallel}$ to obtain (84), and putting the resulting diffusion tensor as defined by (85) into (90). We do not need to evaluate (89) further than to note that it has unit area and width of the order of $\hat{\omega}$. This width is explicitly

$$\hat{\omega} = \left\{ \frac{\pi}{6}\,\frac{q^2}{m^2}\,\frac{k_{\parallel}^{\,4} v_{\perp}^{\,2}}{\omega^2}\,\Big[\dot{\varepsilon}(\omega_{ci})\Big]_{v_{\parallel}} \right\}^{1/3} \tag{91}$$

and is a function of $v_{\perp}$ as well as of $v_{\parallel}$. To estimate when the broadening becomes important, replace $v_{\perp}^{\,2}$ by $\langle v_{\perp}^{\,2}\rangle$ and consider the spectral energy to be restricted to some frequency interval $\delta\omega$ about ω_{ci} as seen by resonant particles with some parallel velocity $v_{\parallel}$. Also, define the mean square oscillation velocity due to this energy band.

$$\langle v_E^{\,2}\rangle = \langle (qEm/\omega)^2\rangle \tag{92}$$

Then

$$\hat{\omega}^3 = \frac{\pi}{6}\,\frac{k_{\parallel}^{\,4}\langle v_{\perp}^{\,2}\rangle\,\langle v_E^{\,2}\rangle}{\Big[\delta\omega\Big]_{v_{\parallel}}} \tag{93}$$

where $\left[\delta\omega\right]_{v_\parallel}$ is the range of frequencies as measured in the frame of a resonant particle. Any description of the process in Figure (19) which neglects Dupree broadening therefore breaks down when

$$\frac{\pi}{6} k_\parallel^4 \langle v_\perp^2 \rangle \langle v_E^2 \rangle > \left[\delta\omega\right]_{v_\parallel}^4 \tag{94}$$

$$\frac{\pi}{6} \langle v_\perp^2 \rangle \langle v_E^2 \rangle \gtrsim \left[\delta v_\parallel\right]^4 \tag{95}$$

where $\delta v_\parallel$ is the range of resonant velocities covered by the AIC spectral width.

The resonance broadening also has the effect of damping the wave growth. Replace the propagator appearing in the linear dispersion relation

$$\frac{1}{k_\parallel v_\parallel + \omega_{ci} - \omega} \cong \frac{P}{k_\parallel v_\parallel + \omega_{ci} - \omega} + i\pi\delta(k_\parallel v_\parallel + \omega_{ci} - \omega) \tag{96}$$

by a more exact propagator including both a linear growth rate and a diffusion term, say the propagator

$$R(k_\parallel v_\parallel + \omega_{ci} - \omega) \equiv i\int_{-\infty}^{0} dt \quad e^{i(k_\parallel v_\parallel + \omega_{ci} - \omega_r)t} e^{\gamma t} e^{+\omega^3 t^3}$$

$$\cong i\left\{1 + i\gamma\frac{\partial}{\partial\omega} + i\hat{\omega}^3 \frac{\partial^3}{\delta\omega_{ci}^3}\right\} \int_{-\infty}^{0} dt \quad e^{i(k_\parallel v_\parallel + \omega_{ci} - \omega_r)t}$$

$$\cong i \left\{ 1 + i\gamma \frac{\partial}{\partial\omega} + i\hat{\omega}^3 \frac{\partial^3}{\partial\omega_{ci}^3} \right\} \frac{1}{k_{\parallel}v_{\parallel} + \omega_{ci} - \omega_r} \tag{97}$$

Now the AIC dispersion relation from (16) is of the form

$$0 = \underbrace{\frac{k_{\parallel}^2 c^2}{\omega_{pi}^2}}_{\substack{\text{free-}\\\text{space}\\\text{con-}\\\text{tri-}\\\text{bution}}} + \underbrace{\frac{\omega}{\omega_{ci}}}_{\substack{\text{elec-}\\\text{tron}\\\text{con-}\\\text{tri-}\\\text{bution}}} + \underbrace{I(k_{\parallel}, \omega, \omega_{ci})}_{\text{ion contribution}} = D_{lin}(k_{\parallel}, \omega) \quad \text{say} \tag{98}$$

Also ω_{ci} appears in the ion contribution only in the resonant denominator (unfortunately, ω appears also in the relation between $B_{\odot}$ and $E_{\odot}$). Thus, the AIC dispersion relation can be made to include both the finite growth rate and the effect of ion diffusion by writing

$$0 = D_{lin}(k_{\parallel}, \omega_r) + i\gamma \frac{\partial}{\partial\omega} D_{lin}(k_{\parallel}, \omega_r)$$

$$+ i\omega^3 \frac{\partial^3}{\partial\omega_{ci}^3} D_{lin}(k_{\parallel}, \omega_r) - \frac{\omega}{\omega_{ci}} - \frac{k_{\parallel}^2 c^2}{\omega_{pi}^2} \tag{99}$$

The derivative with respect to ω_{ci} includes no self-consistent change in f. In addition to the factor $e^{+\hat{\omega}^3 t^3}$ describing orbit diffusion induced by turbulence, the propagator (97) should also include in the integrand a factor $e^{-\hat{\omega}^2 t^2}$ say which describes average orbit shifts induced by turbulence. These average shifts in particle orbits however, lead only to real shifts[22] in mode frequencies and so are not important for the purposes considered here.

For future work with obliquely propagating waves, we quote here the form of the quasilinear diffusion operator with non-zero $k_\perp$[23]. The real quantities a, b, c are the peak magnitudes of the x-, y-, and z-directed electric fields for the mode indexed by $\vec{k}$ when that mode is normalized to unit average field and $\vec{k}_\perp$ is rotated to lie along the x-axis.

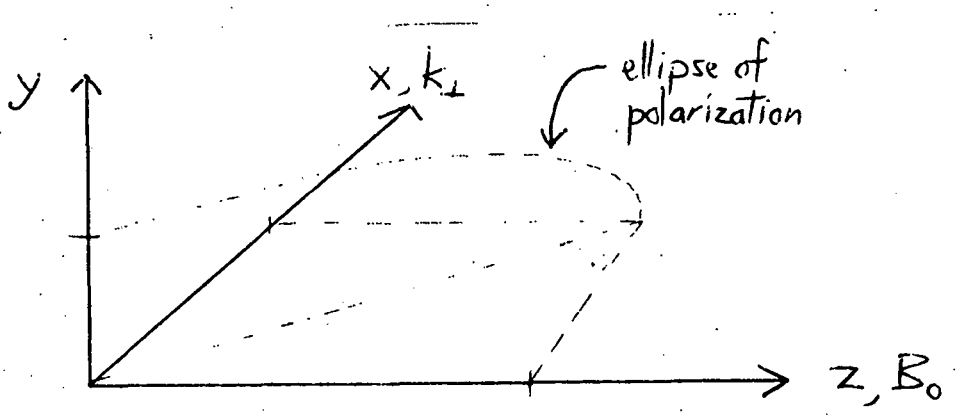

Fig. (20)

$$0 < a$$

$$a^2+b^2+c^2 = 2 \qquad (100)$$

$$\langle E^2 \rangle = 1$$

Wave is circularly polarized in ion sense when a = b = 1, c = 0. If E-vector travels in opposite sense around ellipse, use negative b. If E-vector is located in (+-) x-z quadrant, use negative c. The form of the diffusion equation corresponding to (81) is, including all resonances, and assuming the turbulent spectrum to be symmetric about the k_z-axis,

$$\frac{\partial\langle f\rangle}{\partial t} =$$

$$\frac{\pi}{2}\frac{q^2}{m^2}\int_{0<\omega} d\vec{k}\sum_{\ell=-\infty}^{\infty}\left\{\left[\frac{\omega-k_{\parallel}v_{\parallel}}{\omega}\frac{1}{v_{\perp}}\frac{\partial}{\partial v_{\perp}}v_{\perp}+\frac{k_{\parallel}v_{\perp}}{\omega}\frac{\partial}{\partial v_{\parallel}}\right]\right.$$

$$\left[a\frac{\ell\omega_{ci}}{k_{\perp}v_{\perp}}J_{\ell}+bJ_{\ell}'\right]$$

$$\left.+\left[\frac{\omega-\ell\omega_{ci}}{\omega}\frac{\partial}{\partial v_{\parallel}}+\frac{\ell\omega_{ci}}{\omega}\frac{v_{\parallel}}{v_{\parallel}}\frac{\partial}{\partial v_{\perp}}\right]\left[cJ_{\ell}\right]\right\}\varepsilon(\vec{k})\ \delta(k_{\parallel}v_{\parallel}-\omega+\ell\omega_{ci})$$

$$\left\{\left[a\frac{\ell\omega_{ci}}{k_{\perp}v_{\perp}}J_{\ell}+bJ_{\ell}'\right]\left[\frac{\omega\ k_{\parallel}v_{\parallel}}{\omega}\frac{\partial}{\partial v_{\perp}}+\frac{k_{\parallel}v_{\perp}}{\omega}\frac{\partial}{\partial v_{\perp}}\right]\right.$$

$$\left.+\left[cJ_{\ell}\right]\left[\frac{\omega-\ell\omega_{ci}}{\omega}\frac{\partial}{\partial v_{\perp}}+\frac{\ell\omega_{ci}}{\omega}\frac{v_{\parallel}}{v_{\perp}}\frac{\partial}{\partial v_{\perp}}\right]\right\}\ \langle f\rangle \tag{101}$$

The argument of the Bessel function is $k_{\perp}v_{\perp}\ /\ \omega_{ci}$. The spatial spectral energy density is defined to be the mean square electric field lying in a unit 3-unit dimensional wavevector interval.

$$\varepsilon(\vec{k}) \equiv \Delta\langle E^2\rangle/\Delta^3 k \tag{102}$$

Integrating over $k_{\parallel}$ we obtain the equation corresponding to (84);

$$\frac{\partial\langle f\rangle}{\partial t} = \frac{\pi}{2}\frac{q^2}{m^2}\left(\frac{1}{v_{\perp}}\frac{\partial}{\partial v_{\perp}}v_{\perp},\ \frac{\partial}{\partial v_{\parallel}}\right)\cdot\int_{0<\omega} d\vec{k}\sum_{\ell=-\infty}^{\infty}\left(\frac{\ell\omega_{ci}}{\omega_{\ell}},\ \frac{k_{\parallel\ell}v_{\perp}}{\omega_{\ell}}\right)$$

$$\left[a_\ell \frac{\ell\omega_{ci}}{k_\perp v_\perp} J_\ell + b_\ell J'_\ell + \frac{v_\parallel}{v_\perp} c_\ell J_\ell\right]^2 \frac{\varepsilon(k_\perp, k_{\parallel\ell})}{\left|v_\parallel - \frac{\partial\omega_\ell}{\partial k_{\parallel\ell}}\right|}$$

$$\left(\frac{\ell\omega_{ci}}{\omega_\ell}, \frac{k_{\parallel\ell} v_\perp}{\omega_\ell}\right) \cdot \left(\frac{\partial}{\partial v_\perp}, \frac{\partial}{\partial v_\parallel}\right) \langle f \rangle \tag{103}$$

Here $\omega_\ell = \omega_\ell(v_\parallel, k_\perp)$ and $k_{\parallel\ell} = k_{\parallel\ell}(v_\parallel, k_\perp)$ are fixed by

$$D(k_\parallel, k_\perp, \omega) = 0 \qquad k_\parallel v_\parallel - \omega + \ell\omega_{ci} = 0 \tag{104}$$

The polarizations of these modes are then described by a_ℓ, b_ℓ, c_ℓ, as in (99). Of course, these polarizations have to be found in the course of solving (104).

REFERENCES

1. M. N. Rosenbluth and R. F. Post, Phys. Fluids 8, 547 (1965).

2. R. F. Post and M. N. Rosenbluth, Phys. Fluids 9, 730 (1966).

3. D. E. Baldwin and J. E. Callen, Phys. Rev. Letters 28, 1686 (1972).

4. D. E. Baldwin, H. L. Berk and L. D. Pearlstein, Phys. Rev. Letters 36 1051 (1976).

5. R. C. Davidson and J. M. Ogden, Phys. Fluids 18, 1045 (1975).

6. J. G. Cordey and R. J. Hastie, Phys. Fluids 15, 2291 (1972).

7. R. J. Briggs, Electron-Stream Interactions with Plasmas, M.I.T. Press (Cambridge, 1964).

8. L. D. Pearlstein, D. C. Watson, L. L. Lodestro, Proc. Ann. Meeting on Theoretical Aspects of Controlled Thermonuclear Research, April, 1976, Madison, Wisconsin, talk no. 2C-11.

9. H. L. Berk et al., in Proc. Conf. on Plasma Physics and Controlled Nuclear Fusion (IAEA, 1969), Vol. II, p. 151.

10. M. N. Rosenbluth, private communication, Oct. 1976.

11. T. A. Cutler, private communication, Sept. 1976.

12. R. H. Cohen, Livermore Report UCID - 17158.

13. T. K. Fowler, Livermore Report UCID - 17244.

14. M. A. Rensink and T. A. Cutler, in Proc. Ann. Meeting on Theoretical Aspects of Controlled Thermonuclear Research, April 1976, Madison, Wisconsin, talk no. 1C-15.

15. T. D. Rognlien, H. L. Berk and T. A. Cutler, in Proc. Ann. Meeting of Am. Phys. Soc. - Plas. Phys. Div., San Francisco, Nov. 1976.

16. J. P. Holdren, Nucl. Fusion 12, 267 (1972).

17. J. A. Byers, Proc. Ann. Meeting on Theoretical Aspects of Controlled Thermonuclear Research, April 1976, Madison, Wisconsin, talk no. P2.

18. D. E. Baldwin, Livermore Report UCRL-78406, August 1976.

19. L. D. Pearlstein, private communication, March 1976.

20. See, for instance, R. Z. Sagdeev and A. A. Galeev, Nonlinear Plasma Theory, Chapter II (W. A. Benjamin, New York, 1969).

21. T. H. Dupree, Phys. Fluids 9, 1773 (1966).

22. J. Weinstock, Phys. Fluids 15, 454 (1972).

23. See, for instance, C. F. Kennel and F. Engelmann, Phys. Fluids 9, 2377 (1966).

DISTRIBUTION

tb

Internal

D. V. Anderson	L-387
O. A. Anderson	L-384
T. R. Badura (File)	L-388
D. E. Baldwin	L-388
W. L. Barr	L-383
R. E. Batzel	L-1
H. L. Berk	L-388
D. H. Birdsall	L-384
A. Blum	L-386
J. K. Boyd	L-387
J. A. Byers	L-388
J. Clauser	L-386
F. H. Coensgen (2)	L-382
B. I. Cohen	L-388
R. H. Cohen	L-388
W. C. Condit	L-383
D. Correll	L-387
W. F. Cummins	L-386
T. A. Cutler	L-387
C. C. Damm	L-386
R. S. Devoto	L-388
J. Fink	L-383
J. H. Foote	L-386
T. K. Fowler (2)	L-382
R. P. Freis	L-388
A. H. Futch	L-386
R. K. Goodman	L-386
L. S. Hall	L-388
G. W. Hamilton	L-383
M. A. Harrison	L-382
C. W. Hartman	L-387
W. Heckrotte	L-388
J. R. Hiskes	L-388
J. Holdren	L-386
E. B. Hooper	L-384
R. Hornady	L-386
A. L. Hunt	L-386
B. M. Johnston	L-387
T. B. Kaiser	L-388
L. L. Lodestro	L-387
B. G. Logan	L-386
N. Maron	L-387
B. McNamara	L-388
R. W. Moir	L-383
A. W. Molvik	L-386
R. H. Munger	L-387
M. L. Nelson	L-382
W. A. Newcomb	L-388
W. E. Nexsen	L-386
T. Orzechowski	L-384
J. E. Osher	L-386
L. D. Pearlstein	L-388
G. D. Porter	L-386
R. F. Post	L-386
P. Poulsen	L-384
D. S. Prono	L-306
M. E. Rensink	L-388
T. Rognlien	L-387
J. Sayer	L-387
J. Shearer	L-306
T. Simonen	L-386
B. W. Stallard	L-386
J. J. Stewart	L-387
K. Struve	L-387
C. E. Taylor	L-383
W. C. Turner	L-386
D. Watson (10)	L-388
P. Willmann	L-387
MFE Library	L-387
TID (15)	L-9
TIC, Oak Ridge (27)	

External

Dieter Sigmar
Oak Ridge National Laboratory
P. O. Box Y
Oak Ridge, TN 37830

Abraham Bers
Room 38-260
Mass. Inst. of Tech.
77 Massachusetts Avenue
Cambridge, MA 02139

Toshi Tajima
Physics Department
Univ. of Calif. - Los Angeles
Los Angeles, CA 90024

External Distribution (cont.)

Paul C. Channell
Institute for Advanced Study
School of Natural Sciences
Princeton, NJ 08540

NOTICE

This report was prepared as an account of work sponsored by the United States Government. Neither the United States nor the United States Energy Research & Development Administration, nor any of their employees, nor any of their contractors, subcontractors, or their employees, makes any warranty, express or implied, or assumes any legal liability or responsibility for the accuracy, completeness or usefulness of any information, apparatus, product or process disclosed, or represents that its use would not infringe privately-owned rights.

NOTICE

Reference to a company or product name does not imply approval or recommendation of the product by the University of California or the U.S. Energy Research & Development Administration to the exclusion of others that may be suitable.

Printed in the United States of America
Available from
National Technical Information Service
U.S. Department of Commerce
5285 Port Royal Road
Springfield, VA 22161
Price: Printed Copy $; Microfiche $3.00

Page Range	Domestic Price	Page Range	Domestic Price
001–025	$ 3.50	326–350	10.00
026–050	4.00	351–375	10.50
051–075	4.50	376–400	10.75
076–100	5.00	401–425	11.00
101–125	5.50	426–450	11.75
126–150	6.00	451–475	12.00
151–175	6.75	476–500	12.50
176–200	7.50	501–525	12.75
201–225	7.75	526–550	13.00
226–250	8.00	551–575	13.50
251–275	9.00	576–600	13.75
276–300	9.25	601–up	*
301–325	9.75		

*Add $2.50 for each additional 100 page increment from 601 to 1,000 pages; add $4.50 for each additional 100 page increment over 1,000 pages.

Technical Information Department
LAWRENCE LIVERMORE LABORATORY
University of California | Livermore, California | 94550